

**CATALYTIC PRODUCTION OF PARA-ETHYLTOLUENE
BY ALKYLATION OF MONO-ALKYLBENZENES WITH
ALCOHOLS**

BY

BABATUNDE AZEEZ OGUNBADEJO

A Thesis Presented to the
DEANSHIP OF GRADUATE STUDIES

KING FAHD UNIVERSITY OF PETROLEUM & MINERALS

DHAHRAN, SAUDI ARABIA

In Partial Fulfillment of the
Requirements for the Degree of

MASTER OF SCIENCE

In

CHEMICAL ENGINEERING

MAY, 2015

KING FAHD UNIVERSITY OF PETROLEUM & MINERALS

DHAHRAN- 31261, SAUDI ARABIA

DEANSHIP OF GRADUATE STUDIES

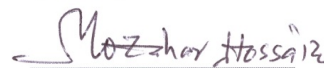
This thesis, written by **BABATUNDE AZEEZ OGUNBADEJO** under the direction of his thesis advisor and approved by his thesis committee, has been presented and accepted by the Dean of Graduate Studies, in partial fulfillment of the requirements for the degree of **MASTERS OF SCIENCE IN CHEMICAL ENGINEERING**.

Thesis Committee



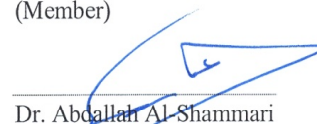
Dr. Sulaiman Al-Khattaf

(Advisor)



Dr. Mohammad Hossain

(Member)



Dr. Abdallah Al-Shammari

(Member)



Dr. Mohammed Ba-Shammakh

Department Chairman



Dr. Salam A. Zummo

Dean of Graduate Studies

21/4/15

Date



Dedicated to

My Late Mum

ACKNOWLEDGEMENT

To begin with, my undiluted gratitude goes to the bestower of knowledge, wisdom and strength, Allaah (azza wajall), for giving me the intellectual and physical capability to complete this M.Sc thesis. All praises is due to you for the gift of life and Islam.

My appreciation goes to my Thesis advisor, Dr. Sulaiman Al-Khattaf, for providing the much needed expertise and enabling environment to actualize the content of this work. The greatest lesson I have learnt under you throughout the duration of this work is that hard work doesn't kill, it only propels towards being a better person.

I would also like to thank my thesis committee members, Dr. Mohammed Hossain and Dr. Abdallah Al-Shammari, for sparing their valuable time and in giving unquantifiable suggestions that added to the depth of this write-up.

My sincere thanks goes to Prof. Jiri Cejka for providing some of the zeolites used in this work, to Dr. A. Aitani for assisting in the manuscript generated from this thesis, to Mr. Mogahid Osman for his contribution in the modelling part and then to Mr. Mariano Gica for spending time with me during the laboratory work.

I am also grateful for the financial support offered towards the completion of this thesis by King Abdulaziz City for Science and Technology (KACST) through Project No. AR-34-22. To all the faculty members, staff and my colleagues in the department of Chemical Engineering at KFUPM, I say, thank you for all forms of assistance rendered to me during my studies.

To my Dad, I say a very big thank you, words alone can't express my gratefulness for your moral and financial support way back from my childhood up to this present moment, if I had drops of water from the world's seas as gift, it can't pay you back. To my aunt, Mrs. Abeni Oworu, I am also indebted for trying your possible best to fill the gap of motherhood.

Finally, I would like to appreciate my siblings, family members, friends, well-wishers, for life would have been unbearable to me without your companionship. Thank you all for your prayers and encouragement.

TABLE OF CONTENTS

ACKNOWLEDGEMENT.....	iv
TABLE OF CONTENTS.....	vi
LIST OF TABLES.....	ix
LIST OF FIGURES.....	x
THESIS ABSTRACT.....	xii
THESIS ABSTRACT (ARABIC)	xiv
CHAPTER ONE.....	1
1.0 INTRODUCTION.....	1
1.1 Background Information on Ethyltoluene.....	1
1.2 Need for P-ET.....	3
1.3 Chemistry of Alkylbenzene Alkylation with Alcohols.....	6
1.4 Zeolites.....	8
1.5 Aims and Objective.....	9
1.6 Scope of Study.....	10
CHAPTER TWO.....	11
2.0 LITERATURE REVIEW.....	11
2.1 Background.....	11
2.2 Alkylation over ZSM-5 zeolite.....	11
2.3 Modified ZSM-5 (by Compounds).....	12
2.4 Modified ZSM-5 (External Surface)	19
2.5 Other Catalyst System.....	21
2.5.1 X and Y Zeolites	21
2.5.2 Beta Zeolite.....	22

2.5.3	Hydrotalcites (HTs) and Aluminophosphates (AIPOs).....	22
2.6	Reaction Mechanism and Kinetic Analysis.....	23
2.7	Findings from Literature Review.....	27
	CHAPTER THREE.....	28
3.0	EXPERIMENTAL SECTION.....	28
3.1	Materials	28
3.2	Catalyst Characterization.....	29
3.2.1	Brunauer-Emmett-Teller (BET) specific surface areas.....	29
3.2.2	X-ray Diffraction.....	29
3.2.3	SEM Images.....	30
3.2.4	NH ₃ temperature-programmed desorption (TPD).....	30
3.2.5	Pyridine FTIR.....	31
3.3	Catalytic Reactions	31
	CHAPTER FOUR.....	
4.0	ALKYLATION OF TOLUENE WITH ETHANOL TO PARA-ETHYLTOLUENE OVER MFI ZEOLITES.....	35
4.1	Introduction.....	35
4.2	Kinetic modeling.....	36
4.3	Results and Discussion.....	41
4.3.1	Catalyst characterization.....	41
4.3.2	Catalytic Activity.....	49
4.4	Kinetic model evaluation.....	59

CHAPTER FIVE

5.0 ZEOLITIC EFFECT IN PARA-ETHYLTOLUENE PRODUCTION

USING DIFFERENT ALKYLATION ROUTES.....	64
5.1 Introduction.....	64
5.2 Results and Discussion.....	65
5.2.1 Zeolites Characterization.....	65
5.2.2 Catalytic Activity.....	71
5.3 Kinetics of Toluene alkylation with ethanol.....	88
5.3.1 Reaction Mechanism.....	88
5.3.2 Model parameter evaluation.....	96
CHAPTER SIX.....	98
CONCLUSIONS AND RECOMMENDATIONS.....	98
6.1 Conclusions from MFI comparative study.....	98
6.2 Conclusions from different zeolites and alkylation routes.....	99
6.3 Recommendation.....	99
NOMENCLATURE.....	101
REFERENCES.....	103
VITAE.....	107

LIST OF TABLES

Table 1.1	Equilibrium composition of ethyltoluene isomers at different Temperatures.....	5
Table 2.1	Activity results of modified ZSM-5.....	14
Table 4.1	Physico-chemical properties of zeolite samples.....	43
Table 4.2	Acid sites characteristics and pyridine sorption data for zeolite samples.....	48
Table 4.3	Catalytic performance of MFI-80, MFI-280 and MFI- 2000 in toluene ethylation with ethanol at 20 s reaction time and 1:1 toluene: ethanol molar ratio.....	50
Table 4.4	Estimated kinetic parameters for toluene ethylation over MFI-280 and MFI-2000.....	61
Table 5.1	Characteristics of the zeolites under study.....	66
Table 5.2	Product distribution for toluene alkylation with ethanol at 20 s reaction time and 1:1 toluene: ethanol molar ratio for TNU-9, SSZ-33 and IM-5 zeolites.....	74
Table 5.3	Product distribution for toluene alkylation with ethanol at 20 s reaction time and 1:1 toluene: ethanol molar ratio for ZSM-5 and MOR-18 zeolites.....	75
Table 5.4	Evaluating effect of external diffusion limitation.....	94
Table 5.5	Evaluating effect of internal diffusion limitation.....	95
Table 5.6	Estimated kinetic parameters for toluene ethylation on different zeolites.....	97

LIST OF FIGURES

Figure 1.1	Conventional polystyrene production route.....	2
Figure 1.2	Different (a) structures of ET isomers (b) alternative alkylation route to polystyrene.....	7
Figure 2.1	Effect of Mg content on reaction activity and selectivity of ZSM-5 to p-ET.....	16
Figure 2.2	Effect of toluene/ethanol ratio on toluene conversion and selectivity's to ET and p-ET over Ti-ZSM-5.....	18
Figure 2.3	TOS dependence of toluene and para-selectivity for parent and silylated HZSM-5.....	20
Figure 2.4	Possible Reaction Mechanism for Toluene Ethylation.....	24
Figure 3.1	Schematic diagram of the Riser simulator and experimental set-up..	33
Figure 4.1	Reaction network of toluene alkylation with ethanol.....	38
Figure 4.2	N ₂ -adsorption-desorption isotherms of MFI-80, MFI-280, MFI-2000 and silicalite-1.....	44
Figure 4.3	XRD patterns of MFI-80, MFI-280, MFI-2000 and silicalite-1...	45
Figure 4.4	SEM images of MFI-80, MFI-280, and MFI-2000.....	46
Figure 4.5	TPD ammonia profiles of MFI-80, MFI-280 and MFI-2000.....	47
Figure 4.6	Effect of temperature on toluene conversion over MFI-80 (◆), MFI-280 (■) and MFI-2000 (▲) at reaction time of 20 s.....	53
Figure 4.7	Effect of reaction time on toluene conversion over (a) MFI-80 and (b) MFI-2000 at 300°C (●), 350 °C (◆) and 400 °C (▲).....	54
Figure 4.8	Product distribution (a) Key products (b) ET isomers different zeolites @ 400 °C and 20 s.....	57
Figure 4.9	Comparison of p-ET selectivity at isoconversion (~14 % toluene conversion).....	58
Figure 4.10	Comparison between experimental data and predicted values for (a) concentration of toluene (▲) and ethyltoluenes (◆) at 400°C (b)toluene conversion % (▲), ethyltoluenes yield % (◆)...	63

Figure 5.1	XRD patterns of (a) IM-5 (b) TNU-9 (c) SSZ-33 (d) ZSM-5....	67
Figure 5.2	SEM images of (a) IM-5 (b) TNU-9 (c) SSZ-33 (d) ZSM-5.....	68
Figure 5.3	Nitrogen adsorption (○) and desorption (●) isotherms of (a) IM-5 (b) TNU-9 (c) SSZ-33.....	69
Figure 5.4	IR spectra of (1) IM-5 (2) TNU-9 (3) SSZ-33, adsorption of pyridine. Region of hydroxyl vibration (A), region of pyridine vibration (B). Before (ba) and after (aa) adsorption.....	70
Figure 5.5	Effect of temperature on toluene conversion over TNU-9 (◆), IM-5 (■), SSZ-33 (▲), ZSM-5 (●) and MOR-18 (⌘) at reaction time of 20 s.....	73
Figure 5.6	Effect of time on Ethyltoluene (ET) yield during toluene ethylation over TNU-9 (◆), IM-5 (■), SSZ-33 (▲), ZSM-5 (●) and MOR-18 (⌘) at Temperature = 300 °C.....	76
Figure 5.7	Effect of temperature on Ethyltoluene (ET) Selectivity during toluene ethylation over TNU-9 (◆), IM-5 (■), SSZ-33 (▲), ZSM-5 (●) and MOR-18 (⌘) at reaction time of 20 s.....	79
Figure 5.8	Effect of temperature on Ethylbenzene conversion over TNU-9 (◆), IM-5 (■), SSZ-33 (▲), ZSM-5 (●) and MOR-18 (⌘) at reaction time of 20 s.....	82
Figure 5.9	Effect of time on Ethyltoluene (ET) yield during ethylbenzene methylation over TNU-9 (◆), IM-5 (■), SSZ-33 (▲), ZSM-5 (●) and MOR-18 (⌘) at Temperature = 300 °C.....	83
Figure 5.10	Effect of temperature on Ethyltoluene (ET) Selectivity during ethylbenzene methylation over TNU-9 (◆), IM-5 (■), SSZ-33 (▲), ZSM-5 (●) and MOR-18 (⌘) at reaction time of 20 s..	84
Figure 5.11	ET-Selectivity for different alkylation route at ~30% aromatic Conversion.....	86
Figure 5.12	P-ET Selectivity for different alkylation route at ~30% aromatic conversion.....	87
Figure 5.13	Simplified Reaction path for toluene ethylation.....	90

THESIS ABSTRACT

Full Name: BABATUNDE AZEEZ OGUNBADEJO

Thesis Title: CATALYTIC PRODUCTION OF PARA-ETHYLTOLUENE
BY ALKYLATION OF MONO-ALKYLBENZENES WITH
ALCOHOLS

Major Field: CHEMICAL ENGINEERING

Date of Degree: MAY 2015

The production of para-ethyltoluene (p-ET) from two alkylation routes; toluene with ethanol and ethylbenzene (EB) with methanol was investigated over MFI zeolites with varying $\text{SiO}_2/\text{Al}_2\text{O}_3$ ratio (80, 280, and 2000) and zeolites with different pore dimensions in a batch fluidized-bed reactor at a temperature range of 250-400 °C, reaction times of 5-20 s and molar feed ratio of 1:1. For the MFI zeolites study, the product distribution exhibited ethyltoluenes as major product with a maximum yield of 26% over MFI-80 with para-ET selectivity of 100% over MFI-2000 compared with 27% and 48% over MFI-80 and MFI-280, respectively. The high para-selectivity over MFI-2000 was attributed to the combined effects of higher $\text{SiO}_2/\text{Al}_2\text{O}_3$ ratio, very weak acid sites and larger crystal size (longer diffusion length). In the alkylation route and zeolite pore dimension studies, toluene ethylation gave higher yield and selectivity to ethyltoluenes over all the zeolites compared to ethylbenzene methylation. The maximum ET yield achieved for toluene ethylation was 13.7 wt.% using IM-5 and ZSM-5 whereas 12.5 wt.% was obtained in EB methylation over SSZ-33. SSZ-33 also gave the highest ET-selectivity of ~50 % due to the combine effect of its 3-D topology and 12- membered ring

(MR) channels. In contrast to ET selectivity, para-ET (p-ET) selectivity obtained was almost the same, ~26 %, irrespective of the zeolite topology or alkylation route. Kinetic studies of toluene ethylation reaction over the zeolites were conducted using power law coupled with Time-on-Stream (TOS) deactivation model. The correlation between the modelled result and experimental data was satisfactory and the activation energy of the various zeolites used for the alkylation of toluene to ET were IM-5 (58.2 kJ/mol) > SSZ-33 (39.7 kJ/mol) > TNU-9 (27.3 kJ/mol) > MOR-18 (20.2 kJ/mol) > ZSM-5 (17.0 kJ/mol).

ملخص الرسالة

الإسم بالكامل:

باباتوندي عزيز أوغونباديجو

عنوان الرسالة:

إنتاج بارا إيثايل تولوين عن طريق ألكلة أحادي ألكايل بنزين مع الكحول في وجود

المحفزات

التخصص:

هندسة كيميائية

تاريخ الدرجة العلمية: مايو، 2015

تمت دراسة إنتاج بارا إيثيلين في وجود المحفز الزوليوتي إم إف أي عن طريقتين. هذه الطريقتين هما عن طريق التلوين مع الإيثانول و عن طريق الإيثايل بنزين مع الميثانول. تم اختبار التفاعل في مفاعل مغلق في وجود عدة تراكيز من كمية الألومينيوم في المادة الزوليوتية (نسبة السيلكا إلى الألومنا $(\text{SiO}_2/\text{Al}_2\text{O}_3)$)، وكذلك ذات مسامية مختلفة في الحجم عند درجات حرارة تتراوح بين 250-400 درجة مئوية. حيث كانت نسب السيلكا إلى الألومينيوم 80، 280 و 2000. مدة التفاعل المختارة كانت بين 5 و 20 ثانية مع إبقاء نسبة المواد المتفاعلة متساوية. من خلال الدراسة على المحفز الزوليوتي إم إف أي، تبين أن الناتج إيثايل بنزين كان المنتج الرئيسي مع عائد عال يصل إلى 26%، و إختيارية يصل إلى 27% لمادة بارا إيثايل تولوين عند استخدام الزيوليت إم إف أي-80 بينما كانت الإختيارية لمادة بارا إيثايل تولوين وصلت إلى 48 و 100% عند استخدام إم إف أي-280 و إم إف أي-2000 بالتتابع. و يعزي ارتفاع الإختيارية في وجود إم إف أي-2000 إلى الآثار المشتركة لارتفاع نسبة السيلكا إلى الألومنا $(\text{SiO}_2/\text{Al}_2\text{O}_3)$ ، ضعف مواقع الحامضية بالإضافة إلى كبر حجم الكريستال (أطول طول انتشار). أما في طريقة الألكلة و حجم مسامية الزيوليت، ألكلة التلوين أعطت أعلى عائد و إختيارية لإيثايل تولوين في وجود جميع أنواع

الزبوليت المستخدمة مقارنة بألكلة إيثايل بنزين. كان العائد الأقصى لمادة الإيثايل تولوين 13.7% باستخدام إي إم-5 و زي إس إم-5 بينما تم الحصول على 12.5% في ألكلة الإيثايل بنزين في وجود الزبوليت إس إم زد-33. كما تبين أن إس إم زد-33 أعطى انتقائية أعلى وصلت إلى 50% لمادة الإيثايل تولوين بسبب الجمع بين تأثير طوبولوجيا ثلاثية الأبعاد و قنواتها ذات الإثني عشر رابطة. في المقابل، نسبة الاختيارية لمادة البار إيثايل تولوين كانت متشابهة في حدود 26% بغض النظر عن طوبولوجيا الزبوليت أو الطريق الألكلة. وقد جرت دراسات الحركية لألكلة التولوين في وجود المحفزات الزبوليتية باستخدام نموذج التنشيط و قانون القوة إلى جانب مدة التفاعل. كان الارتباط بين نتيجة النمذجة والبيانات التجريبية مرضيا، وكانت طاقة التنشيط من مختلف الزبوليت المستخدمة في ألكلة التولوين إلى الإيثايل تولوين أي إم-5 (58.2 كيلوجول/مول) < إس إم زد-33 (39.7 كيلوجول/مول) < تي إن يو-9 (27.3 كيلوجول/مول) < إم أو أر (20.2 كيلوجول/مول) < زد إس إم-5 (17.0 كيلوجول/مول).

CHAPTER ONE

INTRODUCTION

1.1 BACKGROUND INFORMATION ON ETHYLTOLUENE

The alkylation of monoalkylbenzenes (toluene/ethylbenzene) with alcohols (ethanol/methanol) have generated great attention within the last decade considering the vast number of publications on this topic especially the alkylation of toluene with ethanol [1-5]. This can be attributed to the industrial value of the major alkylation product; isomers of ethyltoluene (ET), the para- in particular, which on dehydrogenation forms p-methylstyrene (p-MS), a monomer used in the production of poly-p-methylstyrene (poly-PMS) that can serve as a better substitute for poly-styrene due to its superior properties [2, 4]. Ethyltoluene (ET) is a colourless, flammable liquid with a petrol-like odour which is insoluble in water and belongs to a group of compounds called volatile organic compounds (VOCs).

Most of the world's styrene is synthesized by a two-step process as shown in Fig 1.1. The first step involves alkylation of benzene with ethylene using an acid catalyst to form ethylbenzene (EB) followed by dehydrogenation under vacuum, over an iron oxide catalyst at elevated temperature.

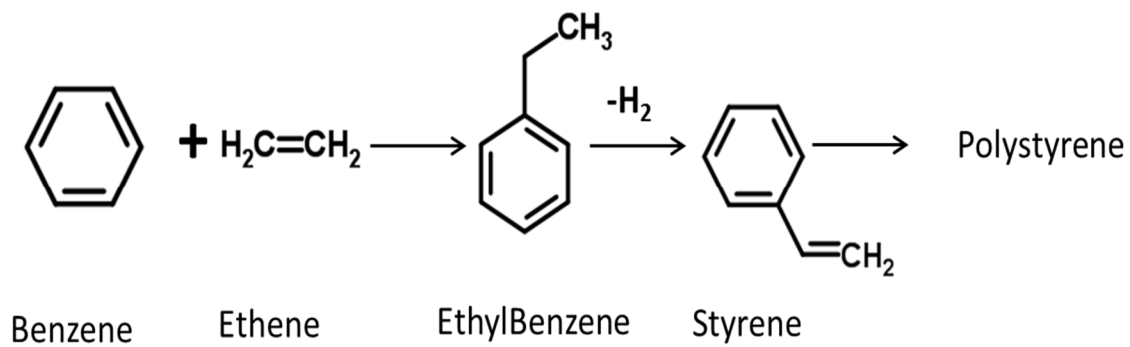


Figure 1.1 Conventional polystyrene production route

1.2 Need for P-ET

The conventional route of styrene synthesis faces numerous reaction limitations such as high cost of feedstock, enormous amount of energy required and emission of greenhouse gases (GHGs) coupled with recent ban on food containers made from poly-styrene in more than 100 major cities due to its classification as carcinogenic by the U.S department of health. Efforts geared towards minimizing these limitations by process optimization and catalyst modification have not yield significant impact thus the need for an alternative to both polystyrene and the reaction route could be found in poly-PMS obtained using toluene/ethylbenzene and ethanol/methanol.

The advantages of poly-PMS over polystyrene are its lower density, giving a 4% reduction in weight required to fabricate a desired product in addition to providing an extra margin of safety for higher temperature use and storage, decrease in moulding cycle time, better mold fill properties, higher melt strength and the fact that its monomer i.e. methylstyrene has not been classified as carcinogenic. The alternative alkylation approach via p-ET opens up a cost effective means compared to styrene due to the utilization of cheaper raw materials and reduction in severe reaction conditions. In order to meet up the world's demand for benzene, about 10% of toluene end use is consumed thus a direct production of p-ET from toluene will eliminate this step from styrene manufacture [6].

For the alternative route to be commercially viable, high p-ET selectivity is desired in contrast to the equilibrium composition which favours the meta- isomer as shown in

Table 1.1. It is also preferable because the boiling points of these isomers are very close and this will give rise to an expensive and complex purification steps.

Table 1.1: Equilibrium composition of ethyltoluene isomers at different temperatures [7]

Temperature (°C)	Equilibrium composition of isomers (%)		
	p-ET	m-ET	o-ET
200	34	53	13
250	33	52.7	14.3
300	32	52.3	15.7
350	31.8	51.4	16.8
400	31	51	18

1.3 Chemistry of Alkylbenzene Alkylation with Alcohols

Ethyltoluenes are diakylbenzenes derived from benzene with replacement of two hydrogen atoms by methyl and ethyl groups and they have a molecular formula C_9H_{12} . The structure of the different isomers of ethyltoluene depending on the position the alkyl group is attached to is shown in Fig. 1.2

Ethyltoluenes can be obtained by three basic methods, i) acid-catalyzed alkylation of toluene with ethylene or ethanol [1-4, 8-12], ii) acid-catalyzed alkylation of ethylbenzene with methanol [13], iii) in small quantity by base-catalyzed side-chain alkylation of toluene with methanol [13]. Only the first two will be investigated in this research work because the third route mainly produces styrene/ethylbenzene. The alkylation of toluene/ethylbenzene with ethanol/methanol produces a wide range of hydrocarbon products which include C_1 - C_4 gases (mostly obtained from dehydration and disproportionation), xylenes, mixture of ethyltoluene isomers and secondary alkylation products such as diethylbenzenes and trimethylbenzenes

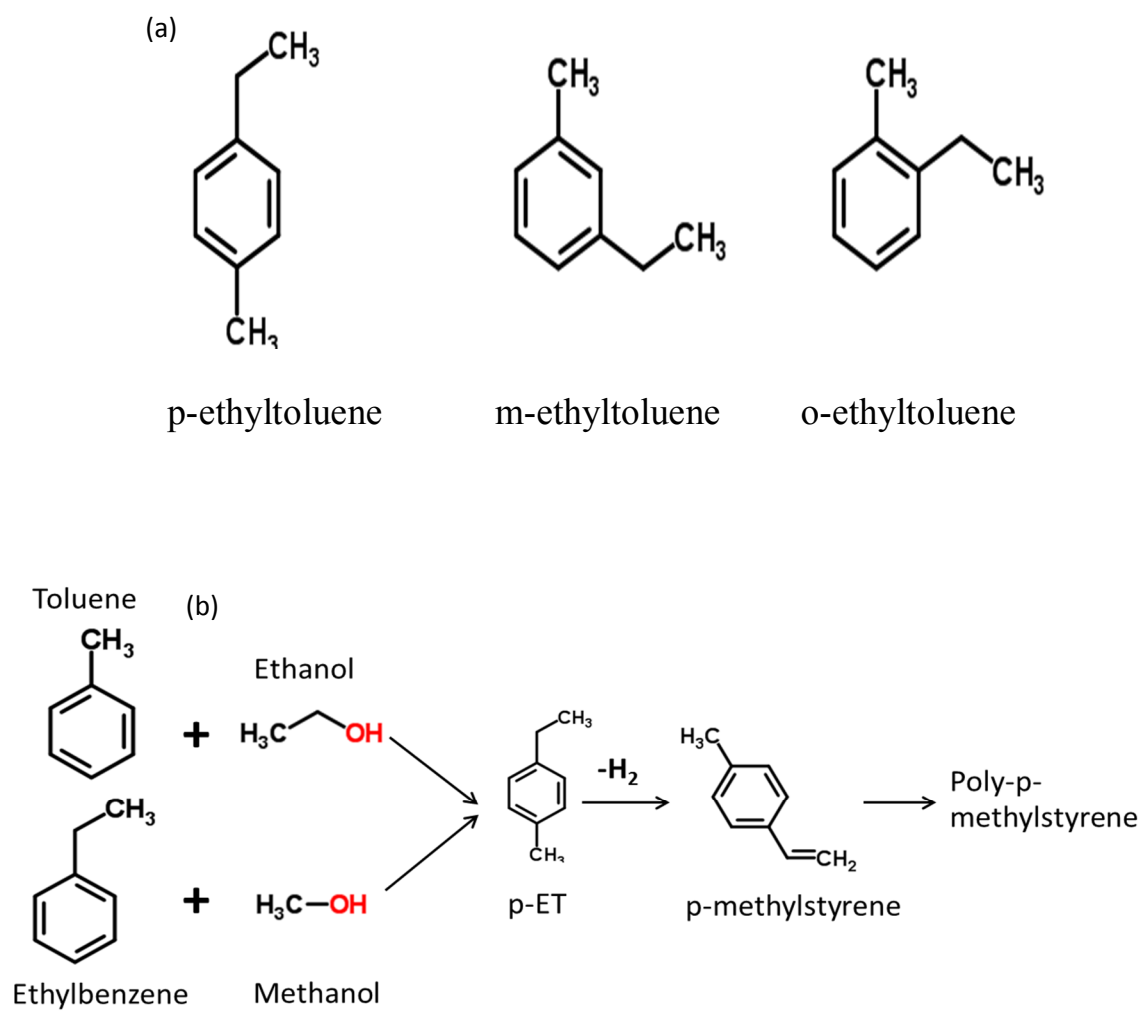


Figure 1.2: Different (a) structures of ET isomers (b) alternative alkylation route to polystyrene

1.4 Zeolites

Zeolites are porous polycrystalline solids with a defined framework, usually multi-dimensional containing silicon, aluminium and oxygen. They have found wide applications in chemical process industries due to their ability to act as molecular sieves based on their pore sizes, ability to preferentially adsorb certain gaseous molecules in gas separation and difference in the diffusion rates of competing molecules within their channel system. More than 200 different zeolite frameworks have been established so far and about 40 occur naturally. The zeolites that are of industrial importance are synthesized because natural zeolites are hardly pure and contaminated by other minerals.

Zeolites can be classified into four types based on their pore sizes; (1) small-pore zeolites containing 8- membered rings (such as zeolite A), (2) medium-pore zeolites having 10-rings in its channel system (e.g. ZSM-5, TNU-9), (3) large-pore zeolites with 12-rings (mordenite, zeolite X and Y) 4) those with 14-rings in their structure called extra-large pore zeolites. The zeolites used in this work are ZSM-5 with different Si/Al ratios, SSZ-33, TNU-9, IM-5, and MOR-18;

SSZ-33 with CON topology has an intersecting 12- and 10- ring channel system, conferring on it some unique characteristics like large void volume and ease of bulky intermediate formation. Its activity in toluene disproportionation and methylation has been studied likewise during xylene isomerization [14]. The structural difference between SSZ-33 and ZSM-5 has also been used to explain the observed product distribution during toluene alkylation with alcohols of varying carbon atoms [14].

TNU-9 (TUN) has a large unit cell size and contains 24 tetrahedral atoms [15] with 10 rings in its intersecting channel systems. It shows some similarity to ZSM-5 (MFI) although the channel intersections in TNU-9 are larger as compared with ZSM-5.

IM-5 (IMF) consists of complex 3-D channel systems, whose structure took a long time before it was disclosed using the enhanced charge flipping technique [16] and with pore dimensions smaller than the 10 rings in ZSM-5. It is a thermally stable catalyst that has been tested in hydrocarbon cracking [17], isomerization of 1-butene [18], for reduction of NO [19, 20] and methanol conversion to hydrocarbons [21].

MOR belongs to large pore zeolites having 12-ring channels (diameter 0.65 x 0.7 nm) and intersecting 8-ring channels (diameter 0.34 x 0.48 nm). It is classified as uni-dimensional because there is no connection between the 12-rings and the pore-width of the 8-rings are too small for most organic molecules to enter [22]. Due to its porosity, it has found wide application in separation of gas mixtures [23] and alkylation reactions [24, 25].

1.5 Aim and Objectives

The aim of this thesis is to selectively produce p-ET from the alkylation reactions of mono-alkylbenzenes (toluene/ethylbenzene) and alcohols (ethanol/methanol). The objectives of this study are to;

1. Modify ZSM-5 (MFI) zeolites or other suitable zeolites for p-ET with improved conversion, yield and selectivity.
2. Evaluate the zeolites performance for the alkylation reactions in a riser simulator (a bench scale fluidized bed reactor).
3. Analyze the effect of zeolite pore structure on p-ET selectivity.

4. Investigate the best alternative alkylation route i.e. toluene with ethanol or ethylbenzene with methanol in terms of p-ET selectivity.
5. Carry out kinetic modelling of the reactions involved in order to build technology knowledge for possible alkylation catalyst scale up.

1.6 Scope of Study

This thesis work will study various zeolites in a bid to understand the relationship between their properties i.e. strength and amount of acid sites, pore structure on p-ET selectivity in the reaction involving toluene/ethylbenzene and ethanol/methanol. The kinetics of the reactions will also be studied using different suitable models i.e. power law and Langmuir Hinshelwood models

CHAPTER TWO

LITERATURE REVIEW

2.1 BACKGROUND

Ethyltoluenes are usually produced via alkylation of toluene with ethanol or ethylene, but another route that has not been reported much in the open literature is via alkylation of ethylbenzene with methanol. In a bid to find a common point for product yield, selectivity and aromatic conversion, several workers have studied conditions that favors formation of ET over different zeolites. At present, no commercial process for the production of p-ET by alkylation of monoalkylbenzenes (toluene/ethylbenzene) with ethanol (ethanol/methanol) exists mainly because of low toluene conversion while maintaining high p-ET selectivity. This attractive route, however, has potential for industrial application if it can be made to selectively form p-ET which can be dehydrogenated to p-methylstyrene.

2.2 Alkylation over ZSM-5 Zeolite

Medium-pore zeolites ZSM-5 has been reported as the most selective catalyst in reactions involving alkylation due to its high activity and low coke formation. In alkylation of toluene with ethanol, ZSM-5 allows the reactant molecules to access the zeolite pores thereby forming a wide range of hydrocarbon products such as C₁-C₄ gases, xylenes, ethyltoluenes, diethylbenzenes (DEB) and trimethylbenzenes (TMB) [4,5,10]. No para-

selectivity was observed over conventional (unmodified) MFI zeolite, instead, the alkylation reaction produces near thermodynamic mixture of ET isomers [1, 26].

Toluene ethylation over ZSM-5 gives a thermodynamic equilibrium composition of ETs: o-ET=16.3%; m-ET= 49.9%, and p-ET = 33.7% at 327 °C [27]. This composition changes with reaction temperature, structural and morphological properties of the zeolites used [8, 28]. o-ET is the largest amongst the three isomers in terms of molecular size and thus, steric effect is more pronounced which obstructs its diffusion out of the zeolite pores. This explains why the yield of o-ET is the least amongst the ET isomers observed on ZSM-5. Neither of the methods described in the literature produces high purity p-ET. Purification requires expensive and complicated separation from two close boiling point components, m-ET and o-ET. Thus, the technical challenge in producing p-ET is technology development to enhance para-selectivity.

Para-selectivity of ZSM-5 has been reported to depend on the nature and strength of the available acid sites, pore size, specific surface area, reaction temperature and toluene to ethanol ratio. The optimal conditions for toluene ethylation were derived using high-silica MFI zeolite and the analysis of empirical process models showed that it was impossible to obtain high selectivity as well as high toluene conversion by change of the process conditions only [5].

2.3 Modified ZSM-5 (by Compounds)

In a bid to improve para-selectivity, several workers have modified ZSM-5 with metal oxides such as Mn, Mg, Cd, P, and Si. Kaeding et al. [29] modified ZSM-5 by impregnation with solutions of phosphorus alongside Magnesium, boron and manganese.

They observed that para-selectivity of ET increased up to 98% with elimination of the o-isomer and a significant decrease of the m-isomer. Modification by metals also showed that the external Brønsted acid sites were reduced, hindering the undesired isomerization of p-ET diffusing out from active sites within the pores. In another study, the acid properties of metals such as Al, B, Fe isomorphously substituted on MFI zeolites decreased as $\text{Al} > \text{Ga} > \text{Fe} > \text{B}$ which were reflected in the activity for toluene conversion [30].

Wang et al. [27] modified ZSM-5 with different contents of Mg and Si by chemical vapor-phase deposition (CVD). The change in the performance of the modified catalyst is shown in Table 2.1.

Table 2.1: Activity results of modified ZSM-5 [27]

Performance of HZSM-5 modified by impregnation method

Conditions	unmodified HZSM-5	4% Mg/HZSM-5	10% Si/HZSM-5
Temperature (°C)	300	350	351
(WHSV) C ₂ H ₄	0.26	0.40	0.43
(Toluene/C ₂ H ₄) mole	9.3	9.8	9.2
C ₂ H ₄ conversion (%)	93.3	72.3	78.4
ET selectivity (%)	71.0	81.1	87.5
Distribution of ET isomers (equilibrium value at 327°C)			
<i>p</i> -ET (33.7) (%)	32.1	72.5	43.1
<i>m</i> -ET (49.9) (%)	65.4	27.3	56.9
<i>o</i> -ET (16.3) (%)	2.5	0.2	0

It was also reported that the method of modification could affect catalyst performance. ZSM-5 modified by impregnation of a magnesium solution showed high ET selectivity (Fig 2.1) compared to the unmodified catalyst but it lost its activity after regeneration which makes it not to have any commercial value. A better method of modification is by CVD and the amount of Si needed to be deposited in order to achieve 99% para-selectivity depends on the crystal size. In a related study, it was discovered that the incorporation of B into ZSM-5 partly filled its porous structure and changed its acidity. The selectivity to p-ET reached 90.80% at 22.92% conversion and the stability of the modified catalyst was also satisfactory.

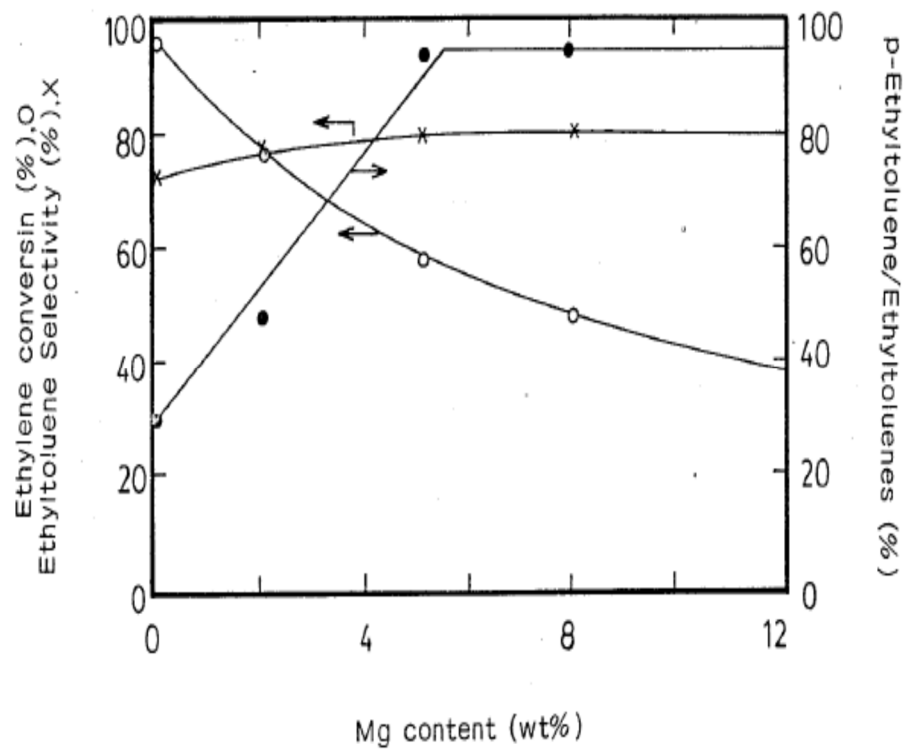


Figure 2.1: Effect of Mg content on reaction activity and selectivity of ZSM-5 to p-ET [26].

Wichterlova and coworkers [31] studied the use of Fe, Mn and Al ion-exchanged H-ZSM-5 zeolites exhibited high para-selectivity during ethylation of toluene. They concluded that metal cations could alter the rates of competitive reactions but did not have a significant influence on the steric hindrances, which is very noticeable with heavier diethylbenzenes.

Ban et al. [32] compared the performances of Ti-ZSM-5, H-ZSM-5 and Mg-ZSM-5 for toluene alkylation using ethanol. The highest p-ET yield was obtained at 350 °C with higher toluene to ethanol ratio and short contact time so as to suppress side reactions. Ti-ZSM-5(with 1% Ti) prepared using Ludox silica showed better para-selectivity compared to pure ZSM-5 and more gave higher resistance to deactivation caused by carbonaceous deposit. The presence of titanium in the ZSM-5 framework significantly reduced both amount and strength of the available acid sites resulting in improved p-ET selectivity as shown in Fig. 2.2. Platinum-exchanged ZSM-5 have also been studied during toluene alkylation using ethane as the alkylating agent but the competing reaction between dehydroalkylation and disproportionation caused a low yield despite high toluene conversion.

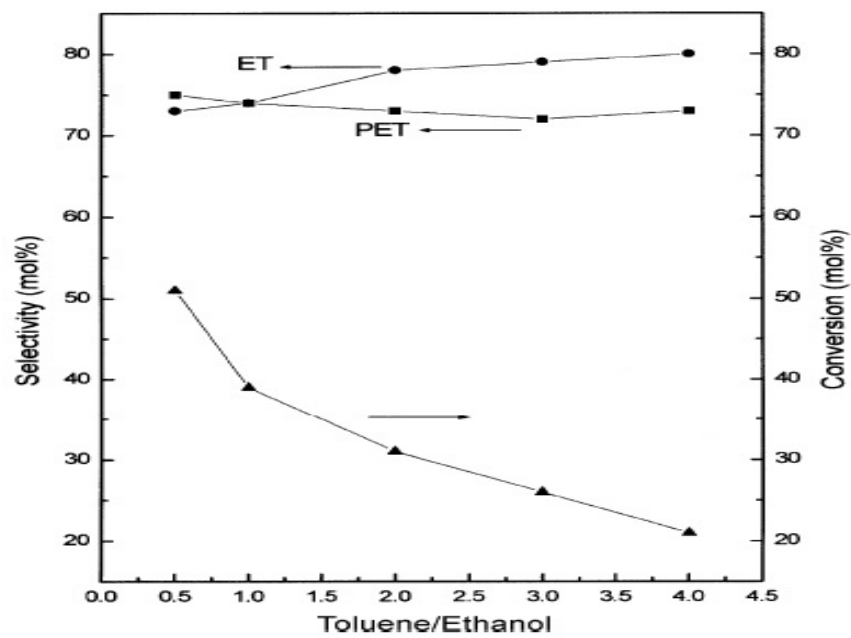


Figure 2.2: Effect of toluene/ethanol ratio on toluene conversion and selectivity to ET and p-ET over Ti-ZSM-5 [32].

2.4 Modified ZSM-5 (External Surface)

From the findings that available acid sites on the external surface area might be responsible for isomerization of p-ET into the other isomers, various researchers have looked into passivating of ZSM-5 zeolite using bulky organosilicon compounds on the external surface so as to enhance para-selectivity. Some of the post synthesis modification methods include both vapor and liquid chemical deposition (CVD/CLD) of silica on the outer surface of ZSM-5. Silylation usually give rise to reduction in the pore size by deposition of tetra-ethoxysilane (TEOS) molecules in the pore entrance and also covering the available acid sites on the external surface. CVD of TEOS molecule covers the non-selective active sites at the external surface, while the internal structure remains unaltered. It was concluded that alkylation of toluene using ethanol over ZSM-5 modified by CVD of silica showed superior activity to that modified by the conventional impregnation with Mg or Si [33].

Čejka et al. [34] have studied the effects of post-synthesis silylation and coke deposition on toluene conversion and product selectivity. The effect of coke deposition apparently showed a rise in p-ET selectivity but when compared at isoconversion of toluene, the p-ET was seen to be lower. Under extreme reaction conditions when coking caused a substantial decrease in toluene conversion, nearly no increase p-ET selectivity was noticed. Contrary to the observation made using coke deposition, silylation on the other hand showed a significant increment in p-ET selectivity. This was attributed to a reduction in the rate of transport for ortho- and meta-isomer. Fig. 2.3 depicts the result obtained with parent and silylated ZSM-5.

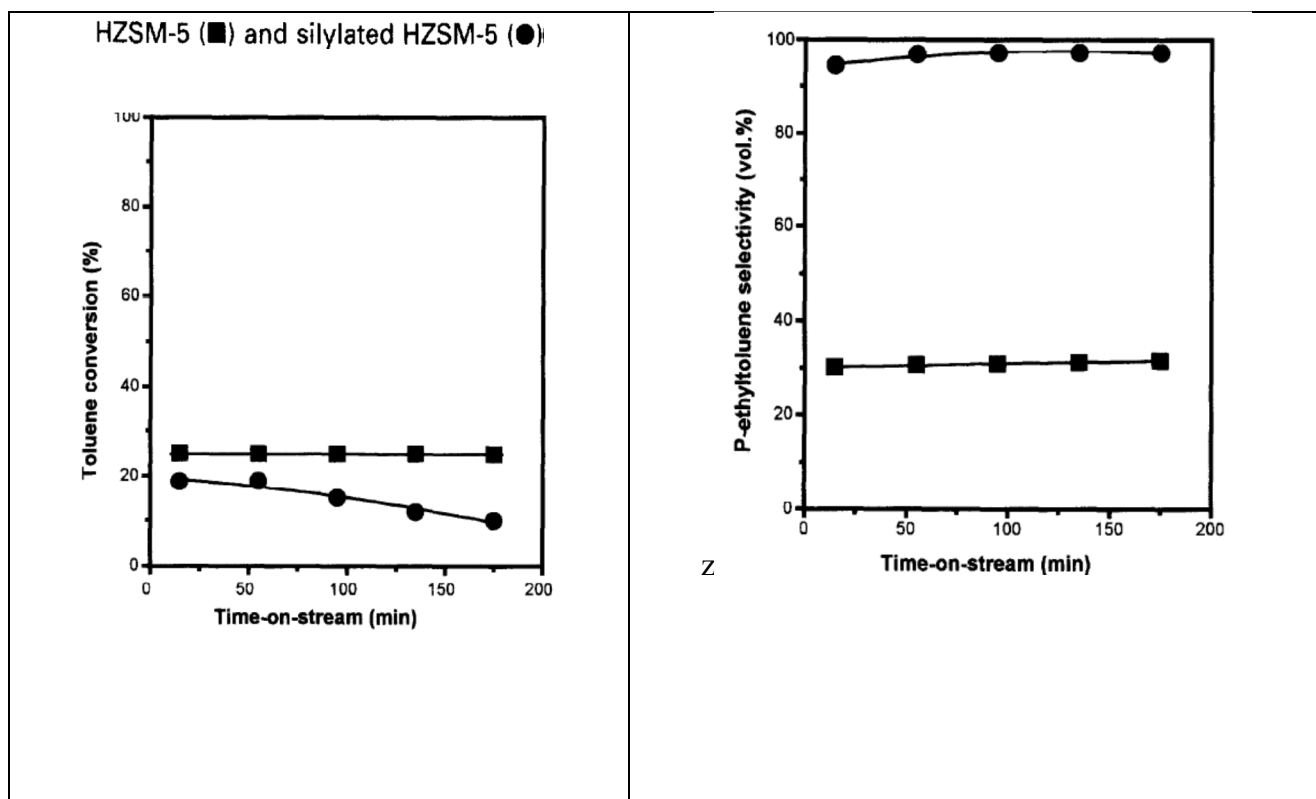


Figure 2.3 TOS dependence of toluene and para-selectivity for parent and silylated HZSM-5 [34].

2.5 Other Catalyst Systems

Apart from ZSM-5, other zeolites that have been investigated in the literature for alkylation of toluene with ethanol and reaction between EB and methanol are given below with some of their findings;

2.5.1 X and Y Zeolites

Coughlan et al. [35] carried out toluene ethylation over NaY zeolite subjected to different extent of cation exchange. They discovered that the number of carbon atoms present in the alkylation agent could alter the degree of unwanted side-reactions and that the extent of cation-exchange did not change the m-ET selectivity. Their findings also indicated that at ion-exchange of about 70 %, the degree of catalyst deactivation and secondary reactions were suppressed and the selectivity to the desired product depends on contact time, calcination and reaction temperature among other factors. They finally concluded that ammonium exchanged Y-type zeolites restricts the diffusion of other aromatics in the product distribution by coke deposition thus enhancing the p-ET selectivity to 65 %.

In another study using USY zeolites and sulfated zirconia (S/ZrO₂) at liquid, near-critical and supercritical conditions with propane as co-solvent, only alkylation reaction was observed over S/ZrO₂ catalyst but competing reactions of alkylation and disproportionation occurred on USY. Working close to or above the critical conditions enhanced product selectivity but severe deactivation was noticed over both catalysts [3].

The alkylation of EB with methanol over X and Y type zeolites was studied under atmospheric pressure and temperature of 400-500 °C. It was observed that ring and side-

chain alkylation took place resulting in the formation of other products such as styrene and methylstyrene, a condition favored by basic zeolites respectively. Over KX, it is believed that the alkylation reaction proceeds by carbonium ion mechanism [13, 36].

2.5.2 Beta Zeolite

For large-pore beta zeolites, it is expected that the extent of steric hindrance which occurs to bulky molecules over medium-pore zeolites will defer. This is evident in the product distribution over beta zeolite comprising of tri- and tetraalkyl derivatives but for ZSM-5, the substituted products are only mono- and di-alkylbenzenes. The catalytic performance of beta zeolite was quite different from that observed over ZSM-5, Romannikov and Ione [7] showed that the ET mixture obtained over beta zeolite contained higher proportion of o-ET.

2.5.3 Hydrotalcites (HTs) and Aluminophosphates (AIPOs)

Hydrotalcite-like compounds contain layered double hydroxides in their structure. They possess anion exchange capabilities due to the weakly bound interlayer anions and this gives them their catalytic properties. Manivannan and Pandurangan [11] studied the performance of calcined hydrotalcites (CHT) substituted with various divalent and trivalent cations such as Al, Mg, Ni, Cu, Co, and Zn in side-chain ethylation of toluene with ethanol at 300-450 °C. MgAl-CHT yielded side-chain alkylated propylbenzene, while over Co, Ni, Cu, and Zn-CHT, side-chain as well as ETs were observed. It was concluded that the combined participation of acidic and basic sites of the CHT-like compounds were found to be crucial for both side chain and ring alkylation of toluene with ethanol.

Aluminophosphates (AlPOs) belong to the group of microporous crystalline materials with neutral frameworks made up of alternating set of AlO_2^- and PO_2^+ . The principal product obtained during vapor phase toluene ethylation over mesoporous aluminophosphate (AlPO) and silicoaluminophosphate (SAPO) molecular sieves was p-ET [37]. This study indicated more free uncondensed -OH groups in pure AlPO that was synthesized using ordered array of cetyltrimethylammonium bromide as structure-directing agent at room temperature. In another study [38], the catalytic performance of isomorphous substitution of Mn(II), Ni(II) and Zn(II) in AlPO-31 molecular sieves (MAPO-31, NAPO-31 and ZAPO-31) was studied for toluene alkylation with ethylene at 300-450 °C. The results showed high toluene conversion over all metal-substituted molecular sieves with m-ET as major product in addition to benzene, styrene, and diethylether. Maximum conversion was achieved at a reaction temperature of 350 °C and a toluene/ethylene ratio of 2. Toluene conversion and m-ET selectivity increased with catalyst acidity, which depended on the structure and the nature of the isomorphously substituted metal ion [39].

2.6 Reaction Mechanism and Kinetic Analysis

Possible reaction mechanisms for alkylation of alkylbenzenes with alcohols have been proposed by different workers [40-42]. Mechanism for toluene ethylation could be suggested as shown in Fig 2.4.

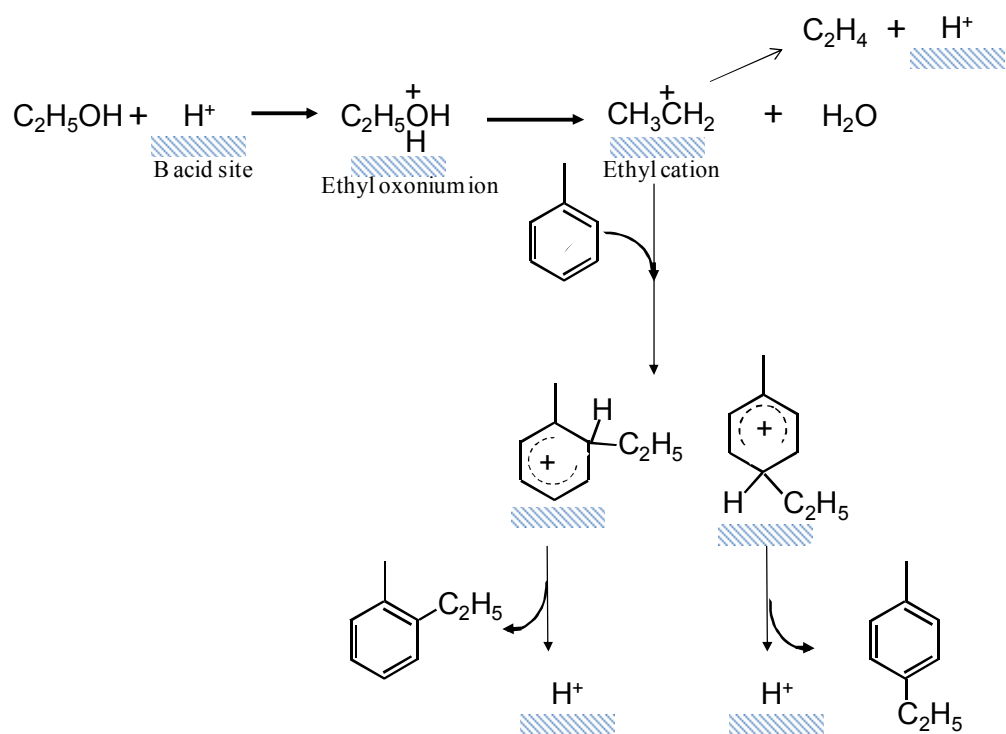


Figure 2.4: Possible Reaction Mechanism for Toluene Ethylation [40].

From the theory of electrophilic substitutions, the electropolar nature of the alkyl group present in an aromatic ring usually determines the position of any incoming substituent group. Those with alkyl groups conferring acidic properties i.e. electronegative groups, directs the new substituent to meta-position while the groups that intensify basic properties such as neutral or electropositive or weakly electronegative groups, directs to ortho- and para- positions [7] but different works on alkylation reactions have shown deviations from the theory of electrophilic substitution in the aromatic ring, with the isomer distribution of products depending on zeolite type, its acidity and reaction conditions [8].

The reaction between toluene and ethanol on ZSM-5 surface needs the alkyl group from the alkylating agent to attach to the aromatic ring instead on the methyl functional group. The methyl group at the aromatic ring activates its ortho- and para-positions for alkylation. However, due to the space restriction within the channels, ethylation occurs mainly at the para-position and p-ET is formed as the primary product which isomerizes to the meta- and ortho-isomers if strong acid sites are available on the external surface [10].

Lee and Wang [27] conducted kinetic analysis of toluene ethylation in a fixed-bed integral reactor at 200-300 °C and atmospheric pressure. It was reported that a noncompetitive model with ethylene adsorption step controlling interpreted the kinetics acceptably well. The activation energy was found to be 18.0 kcal/mol and the heat of adsorption of ethylene was -21.5 kcal/mol. The reaction mechanism proposed from this kinetic study suggested that steric hindrance must be considered in a reaction where large

and small molecules are strongly adsorbed on solid surfaces, especially for the ZSM-5 zeolite with the absence of super cages.

Also, Bhandarkar and Bhatia [43] reported on kinetic study on the selective formation of p-ET was conducted over modified HZSM-5 zeolites in a fixed-bed reactor in the temperature range 300–500 °C and atmospheric pressure in the presence of H₂. The experimental data obtained fitted well with the Langmuir-Hinshelwood mechanism compared to the Eley-Rideal model. The modification of HZSM-5 increased its activation energy from 61.78 kJ/mol (unmodified) to 97.03 kJ/mol (Mg-HZSM-5). The increase was as a result lower acid strength and not to decreased number of acid sites responsible for the alkylation reaction.

Other workers have also investigated the kinetic modelling of toluene ethylation over MFI, proposing that Eley-Rideal and Langmuir-Hinshelwood-Hongen-Watson models gave good fits for the reaction. The heat of adsorption for toluene and ethanol was reported at 56 kJ/mol and 35 kJ/mol, respectively, with surface activation energy of 62 kJ/mol [35]. The adsorption of ethylene over MFI zeolite showed an activation energy of 75 kJ/mol and heat of adsorption of ethylene as 22 kJ/mol [13]. Parikh [30] reported the kinetics of the ethylation reaction using a monolith reactor on which MFI (SiO₂/Al₂O₃ = 24) was wash-coated. A rate expression was proposed which indicates p-ET to be the primary product of the alkylation reaction. o-ET was not considered due to negligible quantities while the net rate of m-ET formation was a result of the total rate of toluene consumption to form p-ET and the subsequent isomerization rate of p-ET to m-ET.

2.7 Findings from Literature Review

From the literature review, the following useful points could be derived:

- Selective production of p-ET by alkylation of mono-alkylbenzenes with alcohols offers several advantages: (i) it produces a negligible quantity of undesired co-products and (ii) cheaper and more abundant feedstocks are used.
- Catalyst used for toluene ethylation with high toluene conversion and p-ET selectivity has not been reported up to now and improving the design of such type of catalysts can expand feed sources for p-methylstyrene and strengthen significantly process economics for the production of poly (p-methylstyrene).
- The key to achieving high p-ET is to eliminate any strong acid sites which is located on the external surface of the zeolite to be used thereby limiting the isomerization reaction of the p-ET formed in the pores to meta- and ortho-isomers.

Alkylation of toluene with alcohols consists of two successive reactions: dehydrogenation of alcohol to form aldehyde and aldol-like reaction of formaldehyde with toluene. Both reactions are catalyzed reactions.

CHAPTER THREE

EXPERIMENTAL SECTION

3.1 MATERIALS

Two of the ZSM-5 zeolites used in this thesis work were procured from Zeolyst; ZSM-5 (CBV8014, NH_4 -form) and ZSM-5 (CBV28014, NH_4 -form). ZSM-5 with a $\text{SiO}_2/\text{Al}_2\text{O}_3$ of 2000 (MFI-2000) was prepared using hydrothermal technique, in a typical synthesis of this sample, 4.26 g tetrapropylammonium bromide, 0.7407 g ammonium fluoride and 0.075 g hydrated aluminum nitrate was dissolved in 72 ml of water and stirred well for 15 min. 12 g silica (381276 Aldrich) was also added and the resulting mixture was well-stirred until a homogenous gel was formed. The obtained gel was autoclaved and kept at 200 °C for 2 days. The molar composition of gel was 1 SiO_2 : 0.08 (TPA) Br: 0.10 NH_4F : 0.0005 Al_2O_3 : 20 H_2O . The solid product obtained was washed with water and dried at 80 °C overnight and the template was removed by calcination in air at 750 °C for 5 h. These zeolites were then referred to as MFI-80, MFI-280 and MFI-2000, where the number represents the nominal $\text{SiO}_2/\text{Al}_2\text{O}_3$ ratio. Silicalite-1 was synthesized by the same procedure as MFI-2000 but without addition of aluminium source i.e. aluminium nitrate. ZSM-5 with nominal $\text{SiO}_2/\text{Al}_2\text{O}_3 = 27$ and mordenite zeolites used in this study was supplied by Zeolyst. The TNU-9, IM-5 and SSZ-33 with their characterization were obtained from the J. Heyrovsky Institute of Physical Chemistry, Prague, Czech Republic.

Prior to catalyst testing, the zeolites were calcined in standing air at 550 °C for 5 h (ramping rate of 3 °C min⁻¹), in order to get the H-form.

All the chemicals used such as toluene, ethylbenzene, ethanol, methanol, tetraethoxysilane, tetrapropylammonium bromide, ammonium fluoride, aluminium nitrate, silica were obtained from Sigma-Aldrich and no further attempt was made to purify them.

3.2 Catalyst characterization

The textural and acid site characteristics of all the zeolites used were analyzed by performing the following methods;

3.2.1 Brunauer-Emmett-Teller (BET) specific surface areas

Among the key parameters in characterizing porous materials e.g. zeolites, are the specific surface area and pore volume. Textural properties were characterized by N₂ adsorption-desorption measurements at 77 K, using Quantachrome Autosorb 1-C adsorption analyzer. Samples were outgassed at 220 °C under vacuum (10⁻⁵ Torr) for 3 h before N₂ physisorption. The Brunauer-Emmett-Teller (BET) specific surface areas were determined from the desorption data in the relative pressure (P/P₀) range from 0.06-0.3, assuming 0.164 nm² for the cross-section of the N₂ molecule. Contribution of micropore and mesopores was derived from the *t*-plot method according to Lippens and de Boer [20]. Whereas, the mesopore size was calculated using the Barret-Joyner-Halenda (BJH) pore size model applied to the adsorption branch of the isotherm [44].

3.2.2 X-ray Diffraction

XRD can be used to obtain various information about zeolite samples such as the average degree of crystallinity which can be calculated from the relative intensities of the peaks produced, the crystallite sizes from the peaks width, presence of amorphous materials using the background of the pattern and the framework of the zeolite when the diffraction

is compared to that of a standard sample. Powder X-ray diffraction (XRD) patterns were recorded on a Shimadzu powder diffraction system using Cu K α radiation ($\lambda = 0.154$ nm, 45 kV and 35 mA). The XRD patterns were recorded in the static scanning mode from 1.2-60 ° (2 θ) at a detector angular speed of 0.01 °/s and step size of 0.02 °.

3.2.3 SEM Images

The morphology and crystal sizes of the MFI zeolites were determined using a scanning electron microscopy (SEM) by Nova NanoSEM FEI with an accelerating voltage of 30 kV.

3.2.4 NH₃ temperature-programmed desorption (TPD)

NH₃-TPD was carried out using Quantachrome Autosorb 1-C/TCD to determine total acid sites on the catalysts. The curve obtained usually consists of two peaks; a low-temperature peak (LT) and a high-temperature peak (HT) representing ammonia desorption from physisorbed (weakly adsorbed) and chemisorbed (strongly adsorbed) acid sites respectively. Samples were pretreated at 450 °C in a stream of helium (25 ml min⁻¹) for 2 h. This was followed by the uptake of ammonia (5 vol. % in helium) at 100 °C for 30 min. The samples were then subjected to flow of helium for 2 h at 120 °C so as to remove loosely bound ammonia (i.e. physisorbed ammonia). After that, the samples were heated from 100-700 °C at a rate of 10 °C/min in a flow of helium (25 ml min⁻¹) while monitoring the evolved ammonia using TCD.

3.2.5 Pyridine FTIR

Infrared spectroscopy of adsorbed pyridine was used to determine the types of available acid sites (i.e. Brønsted and/or Lewis acid sites). The measurements were carried out using a Fourier transform infrared using Nicolet FTIR spectrometer (Magna 500 model). The samples in the form of a self-supporting wafer (ca. 60 mg in weight and 20 mm in diameter) were obtained by compressing a uniform layer of the powdered samples. The wafer was then mounted in an infrared vacuum cell equipped with KBr windows (Makuhari Rikagaku Garasu Inc., Japan), and preheated under vacuum (ca. 10^{-3} torr) at 450 °C for 2 h. The adsorption temperature of pyridine was 150 °C. The IR cell was then cooled down to ambient temperature and placed in an IR beam compartment while under vacuum and transmission spectra were recorded. Desorption of pyridine was also carried out at 350 and 450 °C in order to evaluate the strength of Brønsted and Lewis sites. For a quantitative characterization of acid sites, the following bands and absorption coefficients were used: pyridine (PyH^+) band at 1545 cm^{-1} , $\epsilon = 0.078\text{ cm } \mu\text{mol}^{-1}$; pyridine (PyL) bands at 1461 and 1454 cm^{-1} , $\epsilon = 0.165\text{ cm } \mu\text{mol}^{-1}$ [45-46].

3.3 Catalytic Reactions

Toluene alkylation with ethanol and ethylbenzene with methanol were investigated in a Chemical Reaction Engineering Centre (CREC) fluidized bed reactor (Fig. 3.1) invented by de Lasa [47] using all the zeolites. The reactor consists of two enclosed chambers with a space 800 mg of each catalyst was used with feed molar ratio of 1:1, equivalent to 67:33 wt. % and 77:23 wt. % for toluene/ethanol and ethylbenzene/methanol feedstock respectively, at different temperature levels and time ranging from 200 – 350 °C and 5 – 20 s. Before the commencement of each set of runs, the catalyst was activated for 10 min

at 610 °C in a stream of air followed by reduction of the temperature to the desired reaction level. At the reaction temperature, the impeller fitted to the reactor to cause fluidization was started with a speed of 5500 rpm and 200 ml of the feedstock was injected into the reactor for a desired reaction time. Once the reaction time elapse, the four-port valve opened automatically to ensure termination of the reaction and the product was sent through the pre-heated vacuum box to the gas chromatograph for analysis.

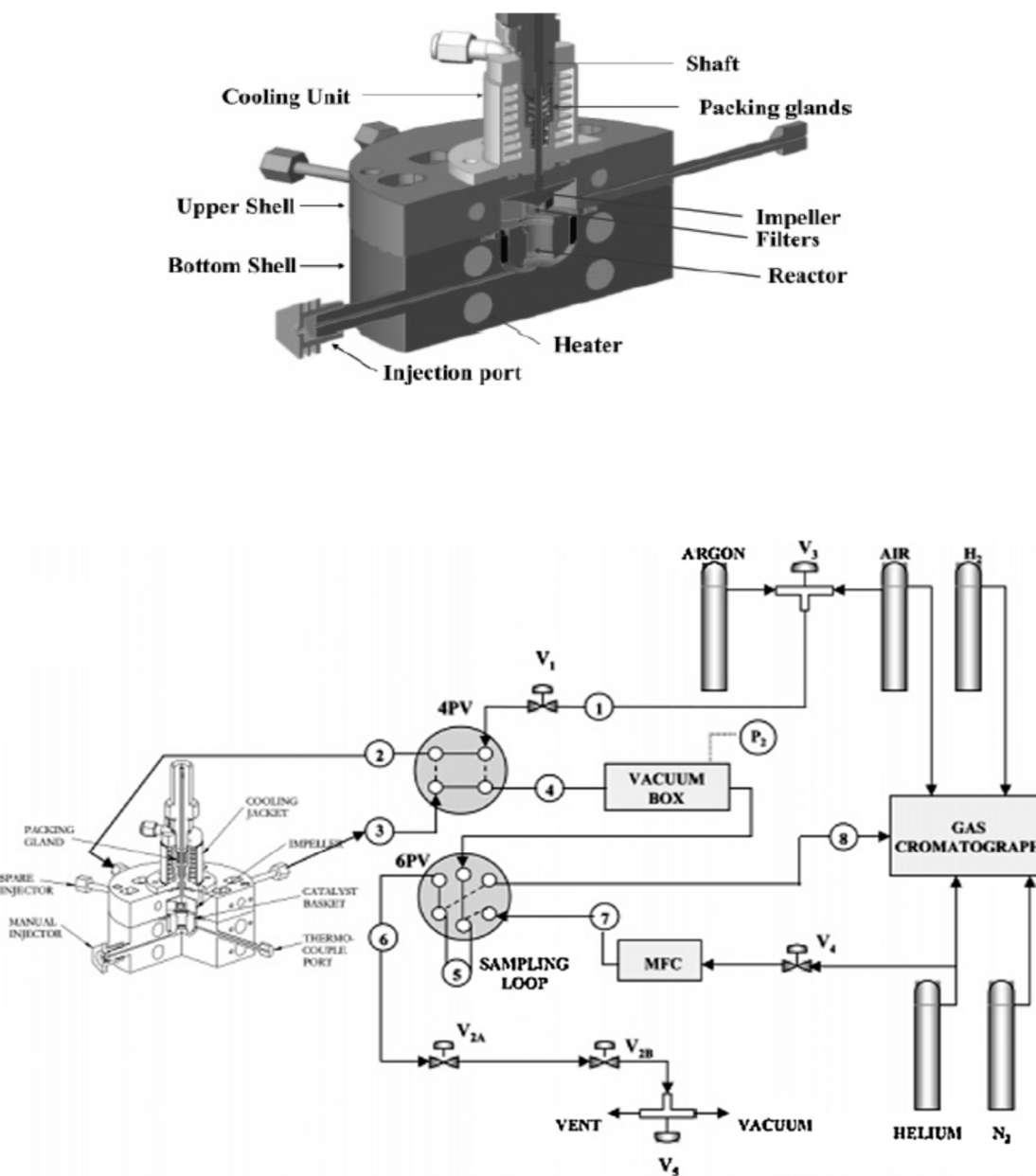


Figure 3.1: Schematic diagram of the Riser simulator and experimental set-up

The product distribution (wt. %) was obtained by multiplying the peak areas from the gas chromatograph with the individual response factors for each component. The response factors were obtained as the slope of calibration curves prepared using different mixtures of known amounts containing compounds present in the products. Each run was repeated to ensure the results can be reproduced with typical deviation in the range of $\pm 2\%$. The conversion, product yield and selectivity were determined using the following relations:

$$\text{Aromatic conversion} = \frac{\text{wt. \% of aromatic converted}}{\text{wt. \% of aromatic fed}} * 100\%$$

$$\text{Yield, \%} = \frac{\text{wt. \% of ethyltoluene}}{\text{wt. \% of aromatic consumed}} * 100\%$$

$$\text{ET Selectivity, \%} = \frac{\text{wt. \% of ethyltoluene}}{\text{wt. \% of aromatics in product}} * 100\%$$

$$\text{para - selectivity, \%} = \frac{\text{wt. \% of para - ethyltoluene (p - ET)}}{\text{wt. \% of ethyltoluene}} * 100\%$$

Measurement of exact amount of each product is difficult in the reaction of (ethanol + toluene) because sensitivities of ethanol and water are different from those of hydrocarbons, and the reaction is accompanied by volume change. The conversion and yield defined above were determined by measuring the gas chromatographic peak areas and using the correction factor on the assumption that the sampling space is constant and the sampling pressure is proportional to the reactor pressure.

CHAPTER FOUR

ALKYLATION OF TOLUENE WITH ETHANOL TO PARA-ETHYLTOLUENE OVER MFI ZEOLITES

4.1 INTRODUCTION

In a bid to make toluene ethylation with ethanol commercially attractive for the production of p-ET, several researchers have investigated various parameters that could enhance activity and para-selectivity. Parikh et al. [30] studied the effects of crystal size and acidity on para-selectivity over Al-MFI and B-, Fe-, Ga-isomorphously substituted zeolites of MFI structure with Si/metal ratios between 50 to 64. They reported that an increase in MFI crystal size results in a reduction in the active sites available on the external surface thereby inhibiting the isomerization of p-ET formed in the pores to other isomers. This is in conformity with the reaction mechanism proposed by Paparatto et al. [28] using MFI ($\text{SiO}_2/\text{Al}_2\text{O}_3 = 25, 58, 63$) and MEL ($\text{SiO}_2/\text{Al}_2\text{O}_3 = 40, 80$). They concluded that p-ET is initially formed in the zeolite channels but undergoes isomerization if there are available acid sites on the external surface [8]. A similar trend on the effect of crystal size on para-selectivity was also observed during the methylation of toluene to p-xylene over MFI [48]. Wichterlova and Čejka [31] studied para-selectivity from the view point of the diffusion coefficient and coke deposition. It was observed that coke deposition did not influence para-selectivity, however, surface silylation with tetraethylorthosilicate (TEOS) could enhance p-ET due to pore narrowing.

Another important factor that could enhance para-selectivity is the external surface area. A correlation has been established between the crystal size and external surface area of

MFI with $\text{SiO}_2/\text{Al}_2\text{O}_3$ ratios of 22 to 600 [31, 49-50]. An increase in the crystal size translates to a reduction in the external surface which enhances the para-selectivity by impeding isomerization into meta and ortho isomers. Further improvement of para-selectivity over MFI can be achieved by impregnation of the zeolite channels with metal or non-metal oxides [30, 43, 51-52]. Modification of MFI ($\text{SiO}_2/\text{Al}_2\text{O}_3 = 50$) with different inorganic additives such as phosphorus, boron and magnesium showed an increase in para-selectivity to p-ET [43]. The best selectivity exhibited by the modified MFI was attributed to a decrease in the strength of the Brønsted acid sites resulting in an increase in the activation energy from 62 to 97 kJ/mol. Chandavar et al. [52] proposed that the addition of P, B and organic bases enhances para-selectivity mainly by suppressing the further isomerization of p-ET to meta-isomer on the strongest acid sites situated at channel intersections.

Most of the zeolites reported in the literature that showed high para-selectivity for toluene ethylation were subjected to post-synthesis steps either by modification of zeolite channels or deactivation of external surface. Consequently, the aim of this section is to present aspects related to the development of a para-selective MFI-zeolite for toluene ethylation to p-ET without the need to modify either the zeolite pore channels or external surface. It deals with the effects of $\text{SiO}_2/\text{Al}_2\text{O}_3$ ratio, crystal size and reaction temperature on p-ET formation. The study also focuses on development of a kinetic model accounting for all reaction steps i.e. adsorption, surface reaction and desorption.

4.2 Kinetic modeling

Phenomenological based kinetic model demonstrating the alkylation of toluene with ethanol is developed based on Fig. 4.1 and the observed data obtained from the fluidized-

bed reactor at different reaction temperatures and varying reaction times. Isothermal reactor condition was assumed given that the amount of the reacting species is relatively small and the contribution of heat of reaction can be considered negligible.

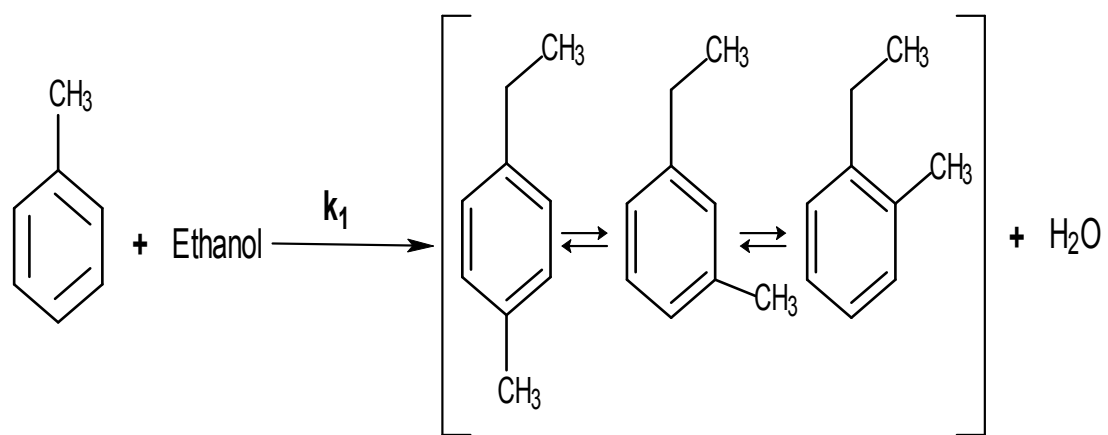


Figure 4.1: Reaction network of toluene alkylation with ethanol.

Within the experimental conditions, the alkylation reactions were considered to be free from internal and external mass transfer limitations. This assumption is reasonable given the fact that the MFI sample used in this study has small crystallite sizes of 0.5 μm to 2 μm . Mentzel et al. [53] also showed similar crystallite size for MFI used in their study. For this crystal size range, one can expect that the value of the effectiveness factor should be close to one. Considering this fact, the effect of diffusion has not been incorporated in the kinetics analysis. Recently, Marin and co-workers [54] reported the kinetic modeling of ethylbenzene dealkylation over Pt promoted MFI catalysts by neglecting the contribution of the diffusion resistance.

Langmuir-Hinshelwood mechanism with surface reaction controlling was proposed as possible kinetics of the reaction of toluene with ethanol. The proposed model considers only the adsorption of ethanol and ethyltoluenes on the catalyst sites, the adsorption of toluene and other products are negligible as compared to ethanol and ethyltoluenes. Ethanol has strong tendency to adsorb on the catalysts' site thereby transforming into surface ethoxy groups which further interacts with lightly adsorbed toluene to form ethyltoluenes [8]. According to the proposed reaction scheme, the rate of toluene disappearance and the rate of ethyltoluene formation can be written as:

Rate of disappearance of toluene (To)

$$-\frac{V}{W_C} \frac{dC_{To}}{dt} = \left[\frac{k_1 K_{EtOH} K_{EtTol} C_{EtOH} C_{EtTol}}{(1 + K_{EtOH} C_{EtOH} + K_{EtTol} C_{EtTol})^2} \right] \phi \quad (1)$$

Rate of ethyltoluenes formation (EtTol):

$$\frac{V}{W_c} \frac{dC_{EtTol}}{dt} = \left[\frac{k_1 K_{EtOH} K_{EtTol} C_{EtOH} C_{EtTol}}{(1 + K_{EtOH} C_{EtOH} + K_{EtTol} C_{EtTol})^2} \right] \varphi \quad (2)$$

where C_i is molar concentration of each species in the system, V is the volume of the reactor, W_c is the mass of the catalyst, t is time in seconds, φ is the apparent deactivation function, k_l is the apparent rate coefficient and K_i is the adsorption coefficient of each species on the catalyst.

The reaction rate constant was represented with the temperature dependence using the following form of Arrhenius equation:

$$k = k_0 \exp\left(\frac{-E}{R} \left(\frac{1}{T} - \frac{1}{T_0}\right)\right) \quad (3)$$

where k_{i0} is pre-exponential factor at the average temperature T_0 and E is apparent activation energy of the reaction.

The adsorption equilibrium constants with the temperature dependence can be expressed according to the following thermodynamic relations [55, 56]:

$$K_i = \exp\left(\frac{\Delta S_{ads,i}^0}{R} - \frac{\Delta H_{ads,i}^0}{R} \left(\frac{1}{T} - \frac{1}{T_0}\right)\right) \quad (4)$$

Where $\Delta H_{ads,i}^0$ is the change of enthalpy and $\Delta S_{ads,i}^0$ is the change of entropy of the adsorption.

The effects of catalyst deactivation has been taken into account by considering a time on stream deactivation function as described in Equation (5) [57].

$$\varphi = \exp(-\alpha t) \quad (5)$$

Where, α is a constant and t is the time the catalyst is exposed to reaction.

A nonlinear regression algorithm (MATLAB, ODE 45-4th order Runge-Kutta method and least-square curve fitting "lsqcurvefit" routine) was used to solve the model equations and to obtain the kinetic parameters. The optimization criteria for the model evaluation are that all the rate constants and the activation energies had to be positive and consistent with physical principles. The details of the regression analysis are described in Waziri et al. [58].

4.3 Results and Discussion

4.3.1 Catalyst Characterization

Table 4.1 shows the SiO₂/Al₂O₃ ratio for the MFI zeolites obtained by AAS analysis. The results showed that MFI-80, MFI-280 and MFI-280 have SiO₂/Al₂O₃ ratio of 86, 295 and 2130, respectively. The nitrogen adsorption isotherms results of the MFI zeolites and silicalite-1 are presented in Fig. 4.2. The textural parameters calculated from the nitrogen sorption isotherms are compiled also in Table 4.1. The surface area of silicalite-1 is 363 m²/g, which is lower than that of other MFI zeolites. The incorporation of Al atoms in the framework increased the pore volume as well as surface area of the material [59]. The total pore volume of MFI-2000 was similar to that of silicalite-1 due to the very low concentration of Al present in MFI-2000.

The XRD patterns of catalyst samples are presented in Fig. 4.3. The patterns of all samples exhibit XRD reflections that conform with the characteristic of MFI structure in the ranges between 8-9° and 22-25° [60, 61]. The intensity of the peaks in the range 22-

25° slightly decreased with an increase in $\text{SiO}_2/\text{Al}_2\text{O}_3$ ratio showing a slight decrease in crystallinity [62].

The SEM micrographs of the three MFI zeolites are shown in Fig. 4.4. MFI-80 has a crystal size of about 0.5-1 μm and MFI-280 has 2-3 μm size, whereas MFI-2000 has a large crystal size of about 30-35 μm . The formation of uniform crystallite for MFI-2000 was also observed.

TPD profiles of desorbed ammonia for the three MFI are presented in Fig. 4.5. The peaks appeared at 300-550 °C correspond to the ammonia desorbed from the acid sites of zeolites whereas the peaks at lower than 300 °C were assigned to ammonia molecules adsorbed either on NH_4^+ species formed on Brønsted acid sites or on Na^+ cations [63]. From the areas of the peaks, the numbers of acid sites were estimated and presented in Table 4.2. The number of acid sites increased with a decrease in $\text{SiO}_2/\text{Al}_2\text{O}_3$ ratio of MFI zeolites, which was expected. Pyridine adsorption by FT-IR spectroscopy was carried out to evaluate the strength and types of acid sites. Table 2 presents the amount of Lewis and Brønsted acid sites in the MFI zeolites. For MFI-80 and MFI-280, the presence of both types of acid sites was observed, whereas in the case of MFI-2000 and silicalite-1 these sites were very weak and were not detected by FT-IR spectra recorded after the adsorption of pyridine and subsequent evacuation at 150 °C.

Table 4.1
Physico-chemical properties of zeolite samples

Zeolite Sample	SiO ₂ /Al ₂ O ₃ ratio ^a	N ₂ sorption			
		d _{spacing} (Å) ^b	S _{BET} (m ² /g)	V (cm ³ /g) ^{c,d}	S _{meso} (m ² g ⁻¹) ^e
MFI-80	86	3.861	425	0.28 (0.19)	68
MFI-280	295	3.856	400	0.23 (0.21)	33
MFI-2000	2130	3.833	367	0.19 (0.18)	5.0
Silicalite-1	∞	3.824	363	0.19 (0.18)	3.0

^a AAS analysis; ^b evaluated by XRD, ^c total pore volume; ^d number in parenthesis corresponds to micropore volume calculated using the t-plot; ^e S_{meso} includes the mesoporous and external surface area

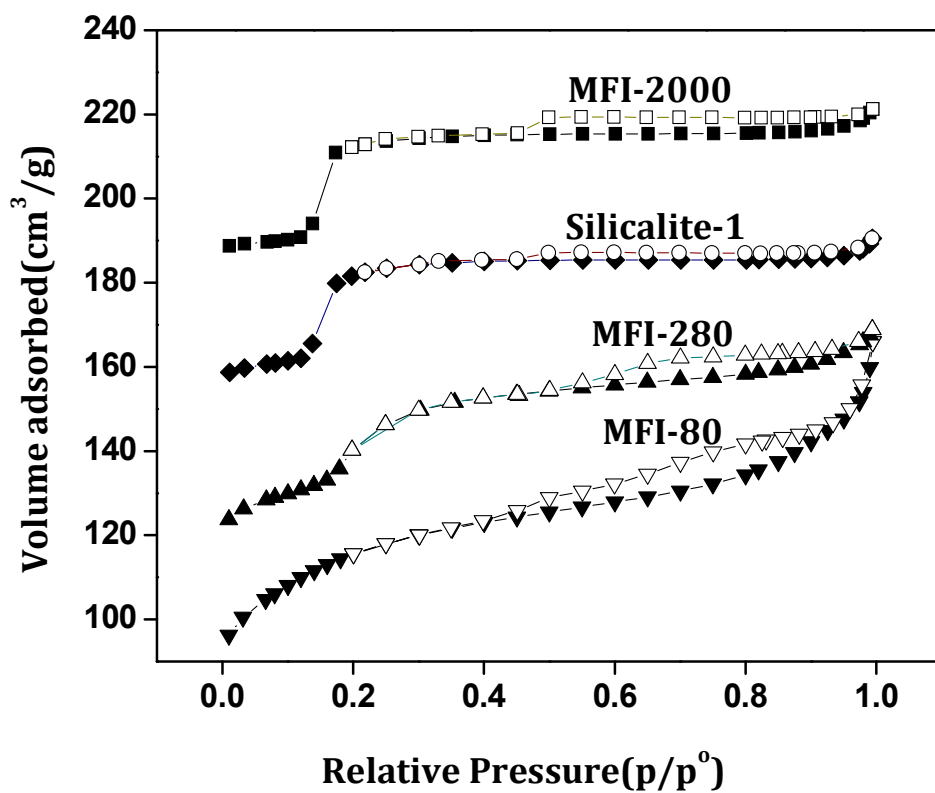


Figure 4.2 N₂-adsorption-desorption isotherms of MFI-80, MFI-280, MFI-2000 and silicalite-1

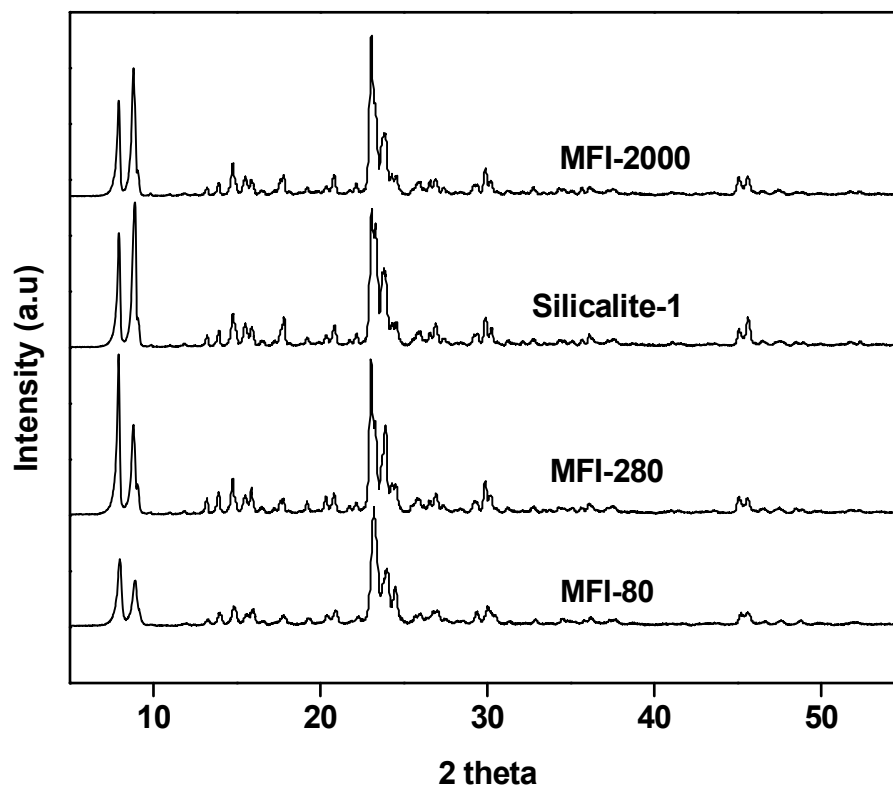
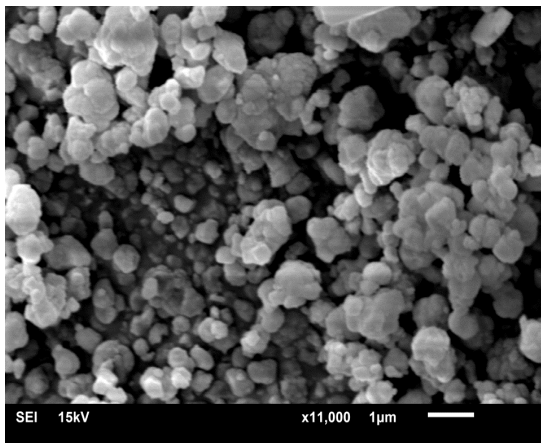
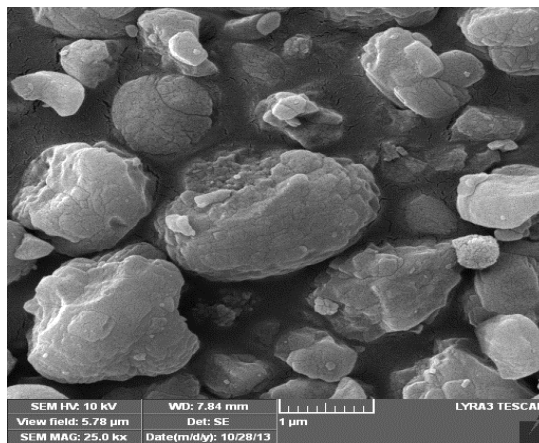


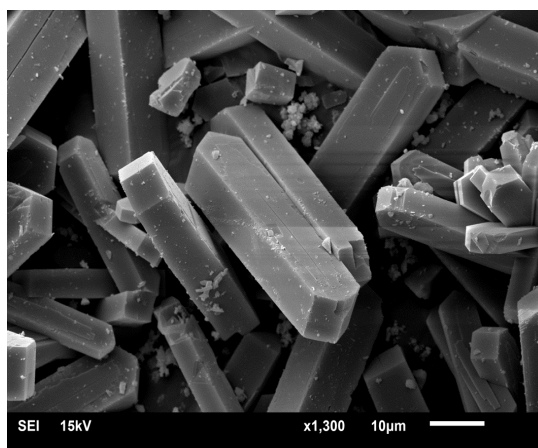
Figure 4.3 XRD patterns of MFI-80, MFI-280, MFI-2000 and silicalite-1



MFI-80



MFI-280



MFI-2000

Figure 4.4 SEM images of MFI-80, MFI-280 and MFI-2000

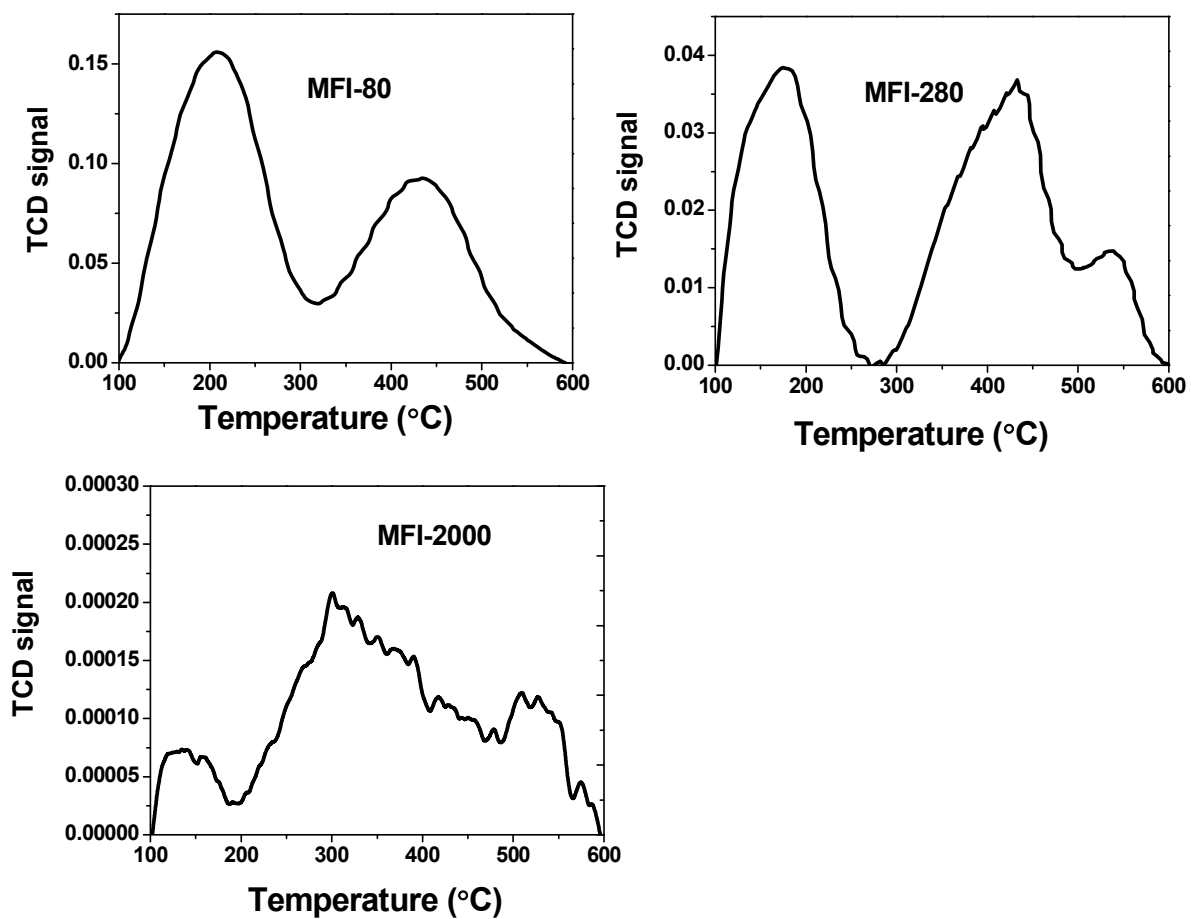


Figure 4.5 TPD ammonia profiles of MFI-80, MFI-280 and MFI-2000

Table 4.2

Acid sites characteristics and pyridine sorption data for zeolite samples

Zeolite Sample	NH ₃ -TPD (mmol g ⁻¹)			Pyridine FT-IR (mmol g ⁻¹) ^a		
	Total Acidity	L.T. < 300 °C	H.T. 300-550 °C	Total Acidity	Brønsted Sites	Lewis Sites
MFI-80	0.16	0.09	0.07	0.14	0.08	0.06
MFI-280	0.07	0.05	0.02	0.02	0.01	0.01
MFI-2000	0.01	0.004	0.006	n.d.	n.d.	n.d.
Silicalite- 1	n.d.	n.d	n.d	n.d.	n.d.	n.d.

^a Absorptivity ratio $\epsilon_{1455} / \epsilon_{1545} = 1.33$ was used to calculate the acidity, TA = total acidity; B = Brønsted acidity; L = Lewis acidity; nd= not detectable; L.T. = Low temperature; H.T. = High temperature, ; n.d. = not detected.

4.3.2 Catalytic activity

Table 4.3 presents the catalytic performance of MFI zeolites for toluene ethylation with ethanol at different temperatures. The results comprise toluene conversion, product yields, and selectivity to ethyltoluenes, p-ET, m-ET, and o-ET. In toluene ethylation over MFI-2000, it is evident that the major product at all temperatures studied was p-ET with trace amount of EB, xylene and benzene indicating a negligible degree of other side reactions such as disproportionation and dealkylation. This is attributed to the low acidity of the catalyst due to its low Al content [25]. The selective formation of p-ET over MFI-2000 may be attributed to the combined effect of acid sites, absence of external acid sites and crystal size. P-ET is formed within the zeolite pores being smaller in size than other isomers and its ease of diffusing over large crystal size in the range of 35-40 μm . The meta- and ortho- isomers are bulkier than p-ET and steric hindrance within the zeolite pore could be expected. P-ET undergoes isomerization at the external surface, subject to availability of Brønsted acid sites, to meta and ortho isomers [8].

Table 4.3

Catalytic performance of MFI-80, MFI-280 and MFI- 2000 in toluene ethylation with ethanol at 20 s reaction time and 1:1 toluene:ethanol molar ratio

Catalyst	MFI-80			MFI-280			MFI-2000		
Reaction Temp. (°C)	300	350	400	300	350	400	300	350	400
Toluene conversion (%)	29.0	29.0	22.2	18.6	22.3	23.8	1.5	8.0	14.2
Product yield (%)									
p-ET	7.3	6.3	3.6	9.4	11.2	8.5	1.5	7.7	13.5
m-ET	16.0	14.2	8.2	4.5	11.1	13.0	-	-	-
o-ET	2.8	3.2	2.1	-	0.3	1.0	-	-	-
Total-ET	26.1	23.7	13.9	13.1	22.6	22.5	1.5	7.7	13.5
Gases	3.9	4.5	7.4	2.5	2.3	2.1	10.8	8.8	7.9
Benzene	0.2	0.8	2.5	0	0	0.2	0	0.04	0.1
Ethylbenzene	0.9	1.5	1.8	0.3	0.6	0.9	0.03	0.1	0.3
Xylenes	0.9	2.0	3.36	0.1	0.5	1.1	0	0.2	0.3
DEBs + TMBs	0.9	0.9	0.7	0.6	0.4	0.3	0	0	0
ET selectivity (%)									
p-ET	27.8	26.4	25.9	67.6	49.6	37.8	100	100	100
m-ET	61.4	59.9	59.3	32.4	49.0	57.7	-	-	-
o-ET	10.8	13.7	14.8	-	1.4	4.5	-	-	-

DEBs = diethylbenzenes, TMBs = Trimethylbenzenes

The formation of m-ET and o-ET isomers over MFI-280 was noticed at the reaction conditions studied. The product distribution over MFI-280 showed a higher quantity of disproportionation products than over MFI-2000. The observed diethylbenzenes (DEBs) over MFI-280 can be attributed to the availability of more Brønsted acid sites (Table 4.2). Over MFI-80, the product distribution became wider indicating significant presence of side reactions such as toluene disproportionation and isomerization yielding benzene, ethylbenzene, xylenes, DEBs and trimethylbenzenes (TMBs).

Ethanol conversion was much higher compared to toluene conversion at all temperatures although the same molar amount of ethanol and toluene was injected as feed. The main reason for higher ethanol conversion is attributed to the alkylation and dehydration reactions which consume additional ethanol molecules. The water molecules formed in alkylation of toluene by ethanol are adsorbed on Lewis acid sites to form protonic acid sites, and on the strong protonic acid sites to form hydronium ions which are weaker acid than the bridged OH groups. Therefore, water molecules might change the type of acid sites (Lewis acid to protonic acid) as well as weaken the protonic acid sites.

4.3.2.1 Effect of temperature

As shown in Fig. 4.6, there is an increase in toluene conversion with the increase in temperature from 300 to 400 °C at 20 s reaction time except that for MFI-80 which showed a reduction in toluene conversion from ~29 % to ~22%. Comparing MFI-80 and MFI-280 at 400 °C, the amount of C₁-C₄ gases for MFI-80 is 3 times more than that of MFI-280. Since these gases are produced from the decomposition of ethanol, it indicates that there is less amount of ethanol available for alkylating toluene to ethyltoluenes over

MFI-80 as shown in Fig. 4.7 (a) and Table 4.3. At 400 °C, the yield of ethyltoluenes over MFI-80 was 13.9% compared with 22.5 % over MFI-280. A similar trend was also observed by Bhandarkar and Bhatia [43] over MFI ($\text{SiO}_2/\text{Al}_2\text{O}_3 = 50$) who attributed it to the decomposition of the alkylating agent and the possibility of reversible reaction within 300-400 °C. However, the increase in the yield of gases with the increase in reaction temperature over MFI-80, contrary to the behavior of MFI-280 and MFI-2000, may be attributed to the high amount of Brønsted acid sites in MFI-80 [7]. In order of strong acid sites, $\text{MFI-80} \gg \text{MFI-280} > \text{MFI-2000}$ so the amount of gases is actually supposed to be in the same order because Brønsted acid sites are known to aid toluene disproportionation and alcohol decomposition but the formation of secondary alkylation products i.e. TMB and DEB and ethylbenzene in the order $\text{MFI-80} > \text{MFI-280} > \text{MFI-2000}$ means some of the gases are being consumed as methyl and ethyl groups. The product distribution for MFI-2000 does not show presence of TMB and DEB thus a significant amount of gases product does not further go into secondary alkylation unlike MFI-80 and MFI-280 which explains why the gases over MFI-2000 is higher at all the temperatures studied.

As the reaction temperature was increased from 300 to 400 °C, the amount of $\text{C}_1\text{-C}_4$ gases produced over MFI-2000 dropped from 10.8 % to 7.9 %. This may be due to the partial consumption of these gases as shown in the product distribution in Table 3. Over MFI-2000, there was an increase in toluene conversion with the increase in temperature at different reaction times but the rapid increase was at a temperature of 400 °C. The maximum toluene conversion obtained was 14 % at 400 °C and a reaction time of 20 s. As the reaction time increased from 5 to 20 s, toluene conversion over MFI-2000 increased drastically especially at 400 °C as shown in Fig. 4.7 (b).

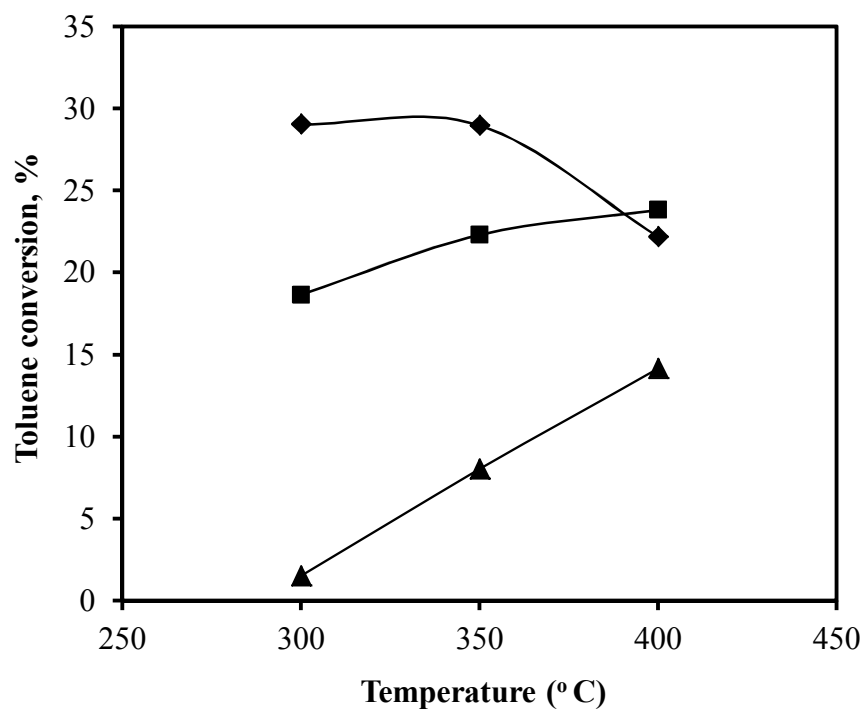


Figure 4.6 Effect of temperature on toluene conversion over MFI-80 (◆), MFI-280 (■) and MFI-2000 (▲) at reaction time of 20 s

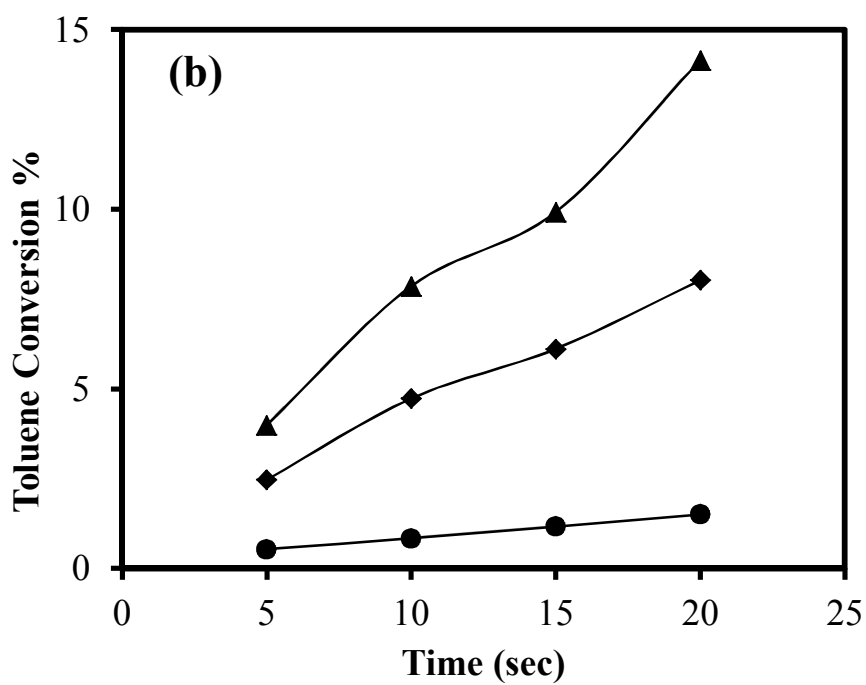
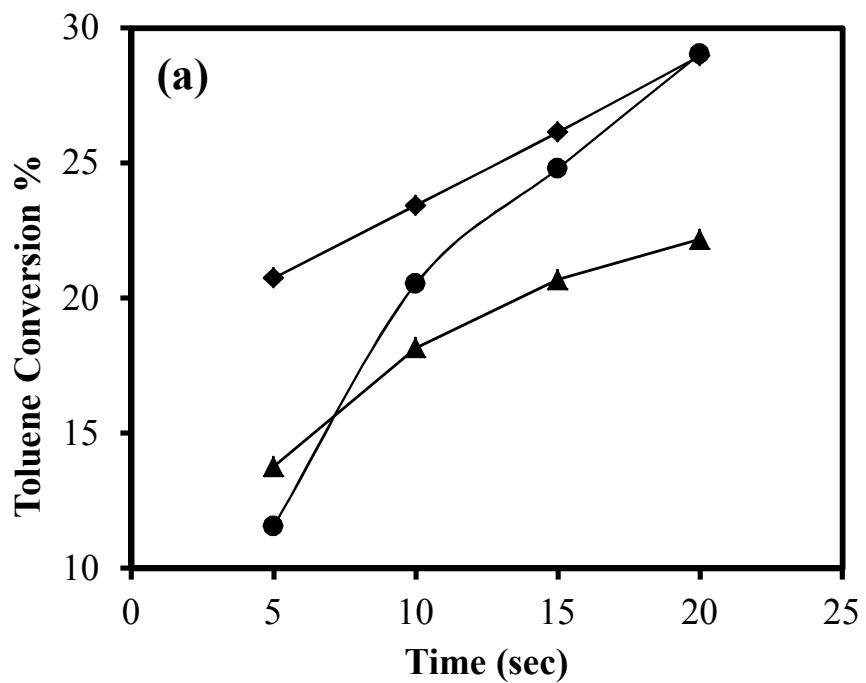


Figure 4.7 Effect of reaction time on toluene conversion over (a) MFI-80 and (b) MFI-2000 at 300°C (●), 350°C (◆) and 400°C (▲).

4.3.2.2 Effect of $\text{SiO}_2/\text{Al}_2\text{O}_3$ ratio

The products that will be focused on are benzene and xylene from toluene disproportionation and the desired alkylation product i.e. ethyltoluene. Other products are in trace amounts and they don't affect the main reaction much. MFI-80 was started with primarily because of its successes that have been reported in selective production of para-diethylbenzene but the disproportionation products were high and the ethyltoluene isomers obtained were similar to the non-selective equilibrium distribution as shown in Fig. 4.8.

The influence of $\text{SiO}_2/\text{Al}_2\text{O}_3$ ratio on the selectivity to p-ET over MFI zeolites is presented in Fig. 4.9 at 400 °C and constant toluene conversion of 14%. The para-selectivity to p-ET for over MFI-2000 was 100% compared with 27% and 48% over MFI-80 and MFI-280, respectively. A similar trend was observed by Al-Khattaf and co-workers [64] after studying the effect of $\text{SiO}_2/\text{Al}_2\text{O}_3$ ratio in diethylbenzenes synthesis over MFI and reported the same phenomenon for para-diethylbenzene selectivity.

It seems that irrespective of the reaction and product obtained over MFI zeolite, an optimum $\text{SiO}_2/\text{Al}_2\text{O}_3$ ratio generally favors para-selectivity [30]. Bhandarkar and Bhatia [9] obtained 56% para-selectivity at a toluene to ethanol ratio of 4:1 over MFI with $\text{SiO}_2/\text{Al}_2\text{O}_3$ of 50, while Paparatto et al. [8] reported 57% para-selectivity with similar feed ratio using MFI with $\text{SiO}_2/\text{Al}_2\text{O}_3$ of 25. The selectivity of the equilibrium mixture obtained over MFI-80 (p-ET 26.4 %, m-ET 59.9 %, o-ET 13.7 %) were in agreement with those reported by Wang et al. over MFI with $\text{SiO}_2/\text{Al}_2\text{O}_3$ of 90 (p-ET 33.7 %, m-ET 49.9 %, o-ET 16.3 %), keeping in mind that the conditions were slightly different [26].

For MFI-80 and MFI-2000, which have high and low concentration of acid sites respectively, variation in temperature did not show any appreciable alteration to their para-selectivity. To elucidate the effect of $\text{SiO}_2/\text{Al}_2\text{O}_3$ ratio, silicalite-1 ($\text{SiO}_2/\text{Al}_2\text{O}_3 = \infty$) was tested for toluene ethylation. It was confirmed that neither activity nor selectivity was observed. At 300 °C and 20 s, toluene conversion was less than 0.4% and yield of ethyltoluenes was 0.2%. From the patterns observed over the three MFI zeolites, it is concluded that optimum $\text{SiO}_2/\text{Al}_2\text{O}_3$ ratio and large crystal size are necessary for maximum para-selectivity to p-ET. However, low $\text{SiO}_2/\text{Al}_2\text{O}_3$ ratio is required for high catalyst activity in the ethylation of toluene.

The results obtained in this study is unique because the toluene to ethanol ratio used was 1:1 in contrast to what is reported in the literature, where high para-selectivity can only be achieved by using higher toluene to ethanol ratio.

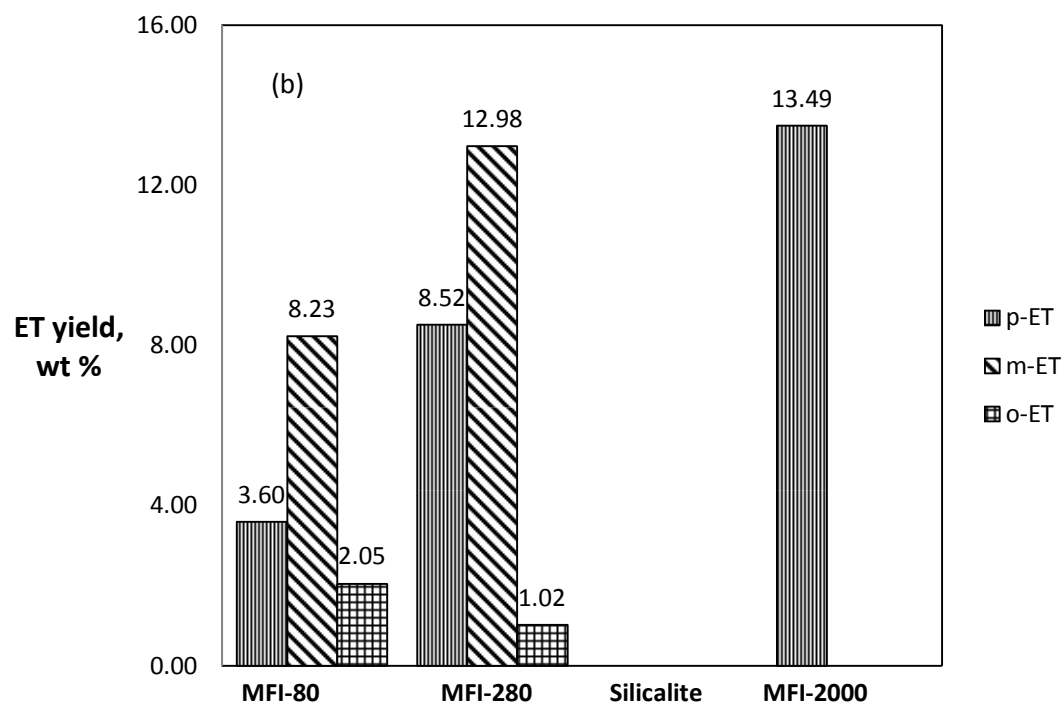
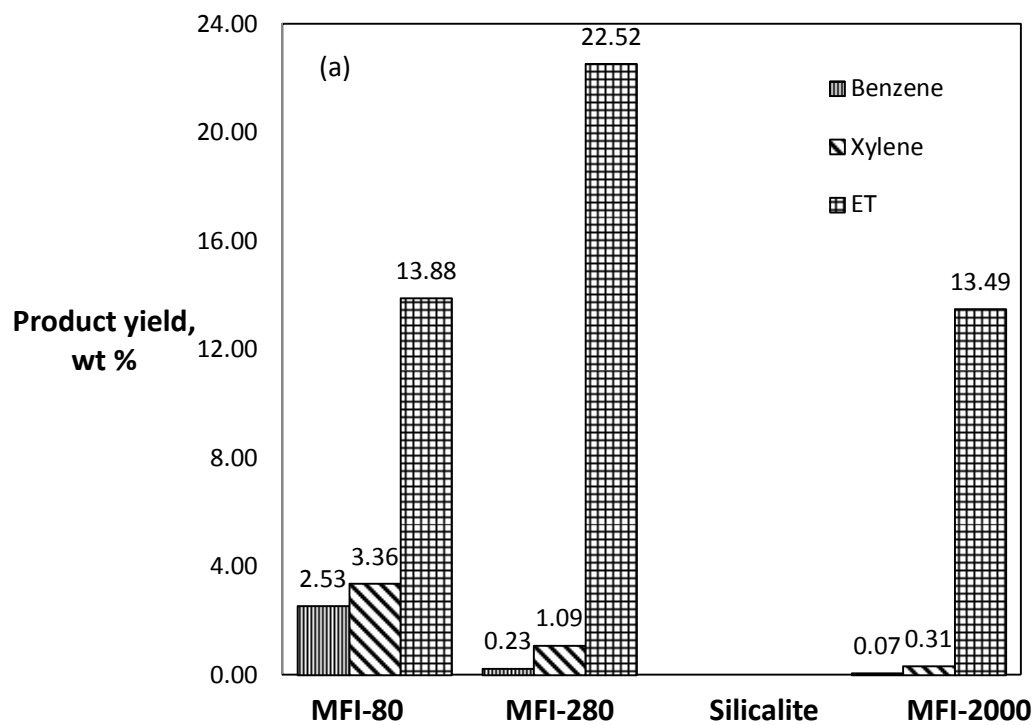


Figure 4.8: product distribution (a) Key products (b) ET isomers different zeolites at 400 °C and 20 s

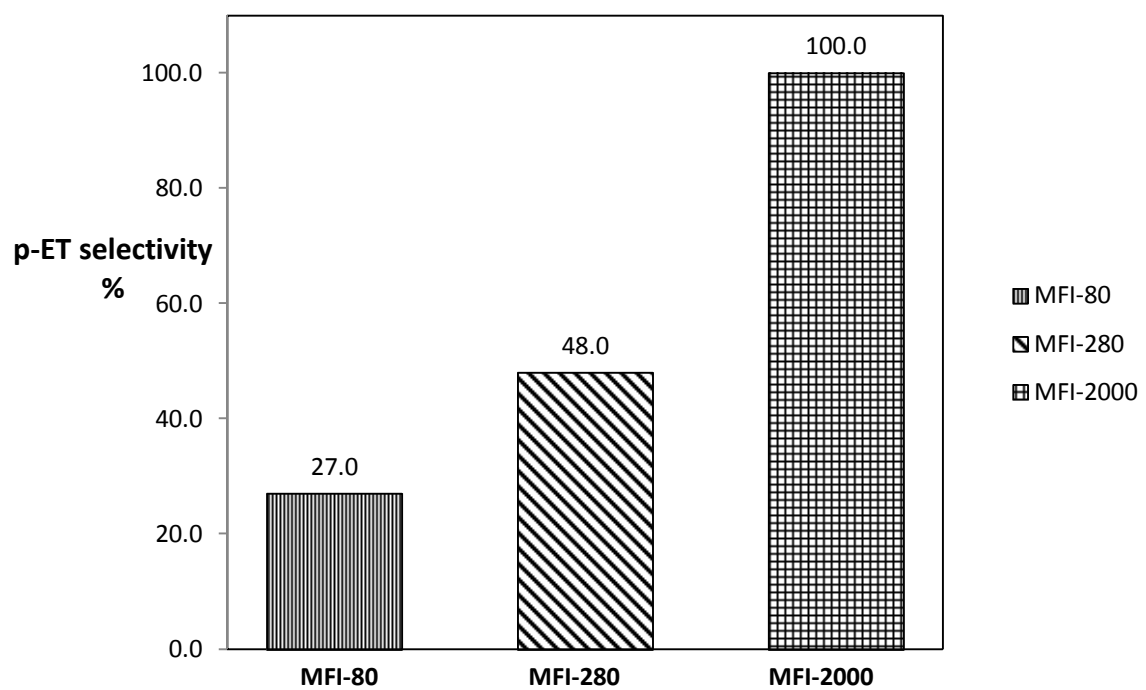


Fig 4.9: Comparison of p-ET selectivity at isoconversion (~14 % toluene conversion)

4.3.2.3 Effect of crystal size

The high para-selectivity observed over MFI-2000 could also be attributed to its large crystal size of 30-35 μm [39]. Beschmann and Riekert [48] investigated the isomerization of xylenes over MFI and concluded that there exists a linear relationship between crystal size and para-selectivity which is pronounced in MFI-2000 zeolite. Arsenova-Hartel et al. [65] proposed an inverse relationship between the rate of isomerization and crystal size of the catalyst in their EB disproportionation study over MFI. They found that high content of p-DEB was noticed over large crystals than smaller ones due to the absence of diffusion limitation. Comparing the product distribution obtained over MFI zeolites, both MFI-80 and MFI-280 yielded appreciable amount of meta and ortho isomers due to their small crystal sizes (short diffusion length) meaning high active sites could be obtained on the external crystal surface. The absence of isomerization over MFI-2000 with higher crystal size gives strength to this assertion.

The effect of crystal size on toluene ethylation showed that the shape selectivity over MFI-zeolites falls under configurational diffusion-controlled selectivity. Chen et al. [66] explained that the differences between transition-state shape selectivity and configurational diffusion selectivity are the factors on which each of them depends, for configurational diffusion selectivity, it is affected by channel diameter and crystal size [67].

4.4 Kinetic model evaluation

Kinetic modeling of the toluene ethylation reaction has been developed based on Figure 4.1 and the equations presented in section 4.2. Langmuir-Hinshelwood model equations (Eq. 1-2) incorporating with the Arrhenius relation, the temperature dependence form of

the equilibrium adsorption constants and deactivation function were simultaneously solved using a nonlinear regression analysis. The details concerning the criteria used for parameters estimation and for the regression analysis are described in the experimental section.

The estimated kinetic parameters and their 95 % confidence limits are shown in Table 4.4. The apparent activation energy (E) obtained from the regression analysis for toluene ethylation over MFI-2000 is more than double (65 kJ/mol) that of toluene ethylation over MFI-280 (30 kJ/mol). This may be attributed to both acidity and diffusion effects. The apparent rate constant for the MFI-2000 is smaller than that of MFI-280 due to the difference in external surface area. This has led to lower activation energy for MFI-280 compared to MFI-2000 [68]. Furthermore the acidity of MFI-280 is about seven times that of MFI-2000 which also has led to a lower activation energy for MFI-280 (30 kJ/mol) compared with MFI-2000 (65 kJ/mol).

Table 4.4

Estimated kinetic parameters for toluene ethylation over MFI-280 and MFI-2000

Parameter	MFI-280	MFI-2000
k_{01} (m ³ /kgcat.s)	0.32 ± 0.01	0.26 ± 0.01
E_1 (kJ/mol)	30.2 ± 8.2	65.2 ± 9.3
- ΔH_{EtOH} (kJ/mol)	19.1 ± 6.2	29.1 ± 5.1
- ΔH_{EtTol} (kJ/mol)	32.7 ± 9.5	21.1 ± 4.2

Al-Khattaf and co-workers showed similar trend for the activation energy for EB ethylation over MFI with varying $\text{SiO}_2/\text{Al}_2\text{O}_3$ ratio [64]. Bhandarkar and Bhatia [9] reported an activation energy of 62 kJ/mol for toluene ethylation over MFI catalyst which is comparable with the results of our study. The estimated adsorption enthalpies for ethanol and ethyltoluenes are also reported in Table 4.4. The results provide an indication for their comparable adsorption strength over both MFI-2000 and MFI-280. Comparing the experimental data with the model predictions, it can be seen from Fig. 4.10 (a) that toluene and ethyltoluenes concentrations predicted by the proposed model fit with the experimental data in an excellent manner. Also for toluene conversion and ethyltoluenes yields shown in Fig. 4.10 (b), accurate match between experimental values and model predictions was obtained. The kinetic study results clearly show that MFI zeolites with different $\text{SiO}_2/\text{Al}_2\text{O}_3$ ratios have a significant impact on the mechanism of toluene ethylation with ethanol.

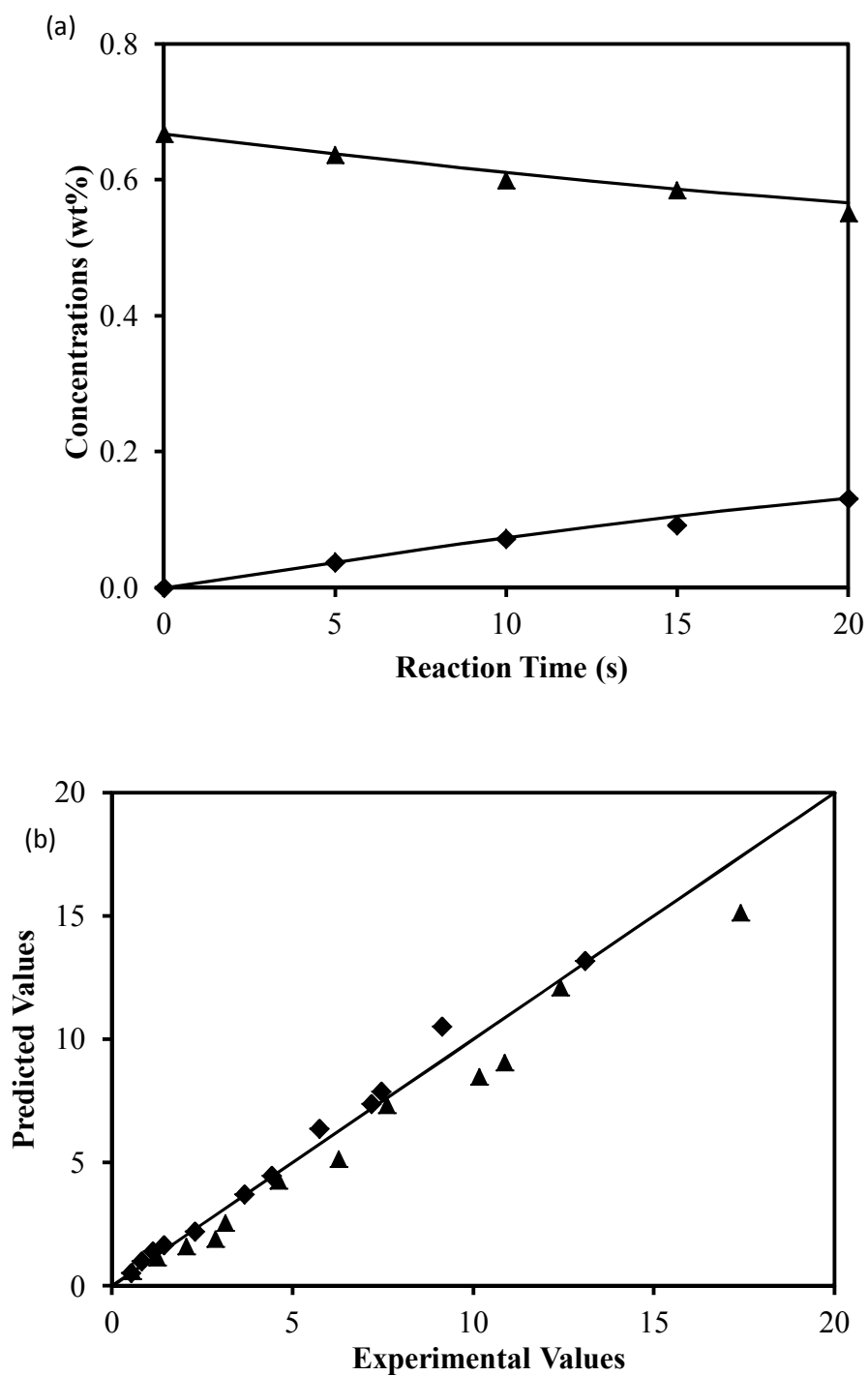


Figure 4.10 Comparison between experimental data (symbols) and predicted values (dotted lines) for (a) concentration of toluene (▲) and ethyltoluenes (◆) at 400°C (b)toluene conversion % (▲), ethyltoluenes yield % (◆)

CHAPTER FIVE

ZEOLITIC EFFECT IN PARA-ETHYLTOLUENE PRODUCTION USING DIFFERENT ALKYLATION ROUTES

5.1 INTRODUCTION

Ethyltoluenes (ETs) are dialkylbenzenes that found a wide use in the petrochemical and chemical industries. In particular is para-ethyltoluene (p-ET), used in the synthesis of poly (p-methylstyrene) which is expected to replace the more carcinogenic polystyrene [69]. The alkylation reaction is usually carried out on medium pore zeolites ZSM-5, to favor para-selectivity, the most desired isomer.

To improve the activity and selectivity of ZSM-5 zeolite, impregnation of the zeolite external surface with metal or non-metal oxides [24, 51, 70] and/or siliceous materials [34, 71] or by carbonaceous material in form of coke deposits [4, 49, 72] have been investigated. Cejka and Witcherlova [49] pointed out the effect of restricted transition-state selectivity during alkylation of toluene with ethylene, which explains how products with smaller intermediates could be favored compared to those with bulky intermediates depending on the pore size of the zeolite. Yao et. al. [72] also established that zeolite topology could play a great role in promoting product selectivity and reaction rates due to the constraints they place on certain molecules and the varying interactions between the pore walls and reactant molecules. Several other factors that can affect activity and selectivity of zeolites have also been studied by different workers such as crystal size [30], amount and strength of acid sites [31, 49-50].

In this section, zeolites with different topology such as SSZ-33, TNU-9, IM-5, ZSM-5 having three-dimensional pore system and MOR-18, possessing large pores are studied in the alkylation of toluene or ethylbenzene with ethanol or methanol respectively to gain an insight to the underlying differences between them.

This section aims to understand the effect of zeolite structures and properties related to the acid-catalyzed formation of ethyltoluenes via two different reaction routes; alkylation of toluene with ethanol and the less reported alkylation of ethylbenzene with methanol.

5.2 Results and Discussion

5.2.1 Zeolites Characterization

The characteristics of all the zeolites used in this study such as pore sizes, Si/Al ratio from chemical analysis, BET area, pore volume and acid sites concentration are shown in Table 1.

The XRD patterns are shown in Fig. 5.1 with the reflections indicating good crystalline structures of the zeolites under study. The SEM images shown in Fig. 2 reveal the morphology of the zeolites and they all have similar crystal sizes in the range of 0.1 – 1.5 μm . As acid sites density is of utmost importance for acid catalyzed reactions, quantitative evaluation of pyridine FTIR spectra showed the Bronsted sites follow the order; MOR-18 > ZSM-5 > TNU-9 > IM-5 > SSZ-33.

Table 5.1 Characteristics of the zeolites under study.

	IM-5	TNU-9	SSZ-33	MOR-18	ZSM-5
IZA ^a code	IMF	TUN	CON	MOR	MFI
Si/Al ratio	21.4	24.4	14.3	24.8	25
Channel	4.8×5.5	5.4×5.5	5.9×7.0	3.4×4.8	5.1×5.5
dimensions (Å)	5.3×5.6	6.0×5.2	6.4×7.0	6.5×7.0	5.3×5.6
Pore topology	3D, 10-rings	3D, 10-rings	3D, 12 and 10- rings	1D, 12 and 8- rings	3D, 10- rings
BET area (m ² /g)	336	420	506	455	357
Pore volume ^b (V _{micro} cm ³ /g)	0.14	0.19	0.20	0.21	0.15
Lewis sites (mmol/g)	0.10	0.12	0.32	0.07	0.10
Bronsted sites (mmol/g)	0.33	0.35	0.19	0.93	0.65

^a International Zeolite Association; ^b obtained from *t*-plot

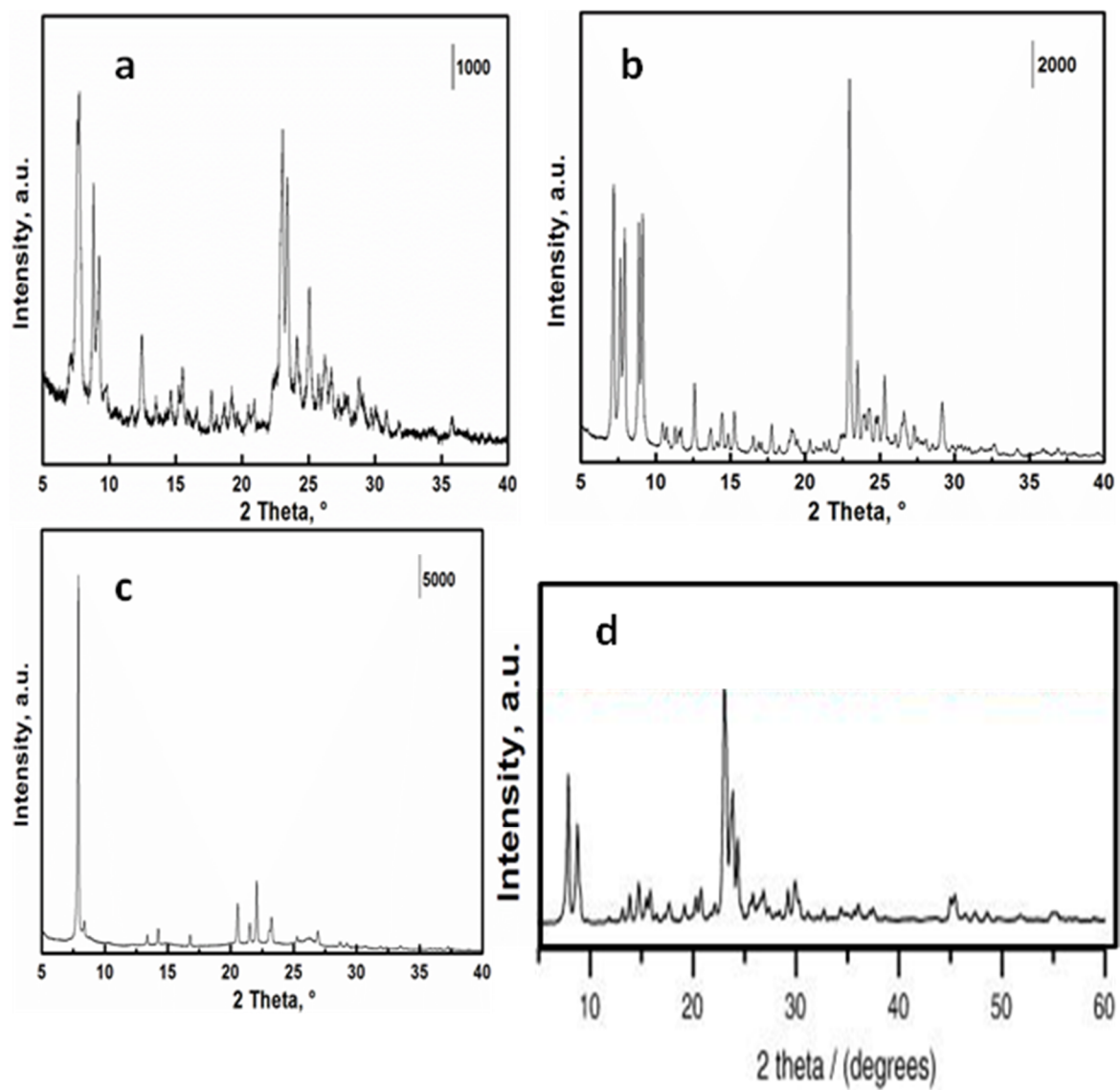


Figure 5.1 XRD patterns of (a) IM-5 (b) TNU-9 (c) SSZ-33 (d) ZSM-5

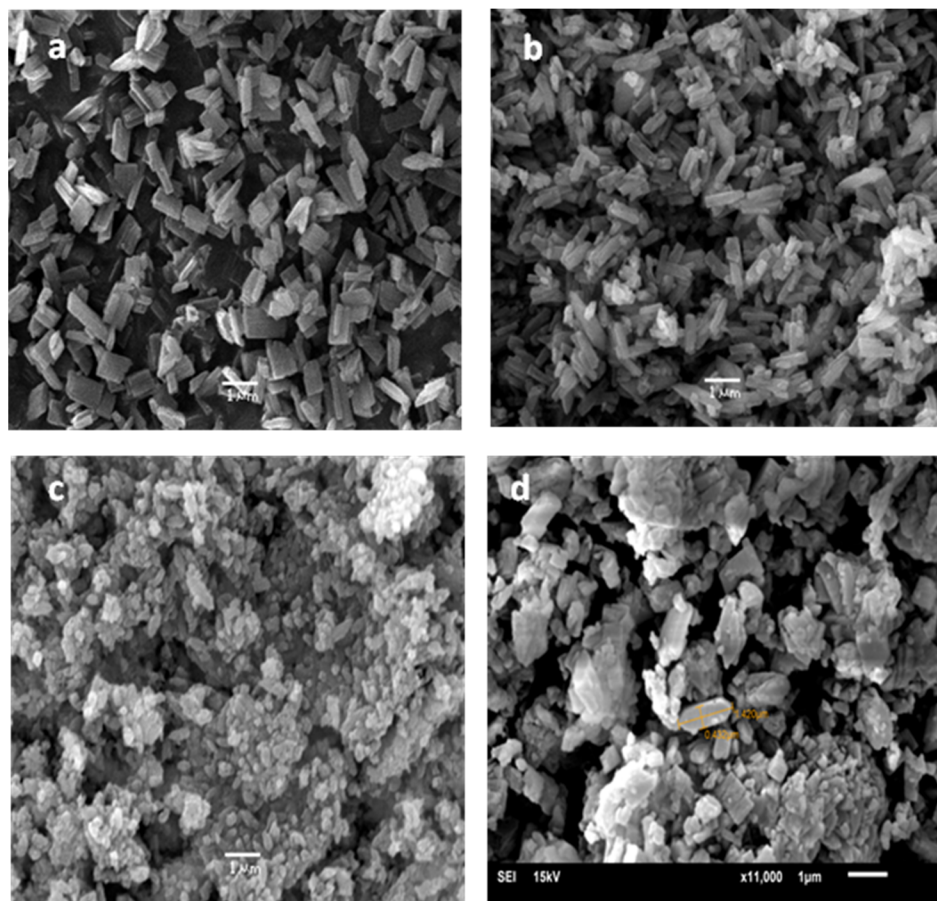


Figure 5.2 SEM images of (a) IM-5 (b) TNU-9 (c) SSZ-33 (d) ZSM-5

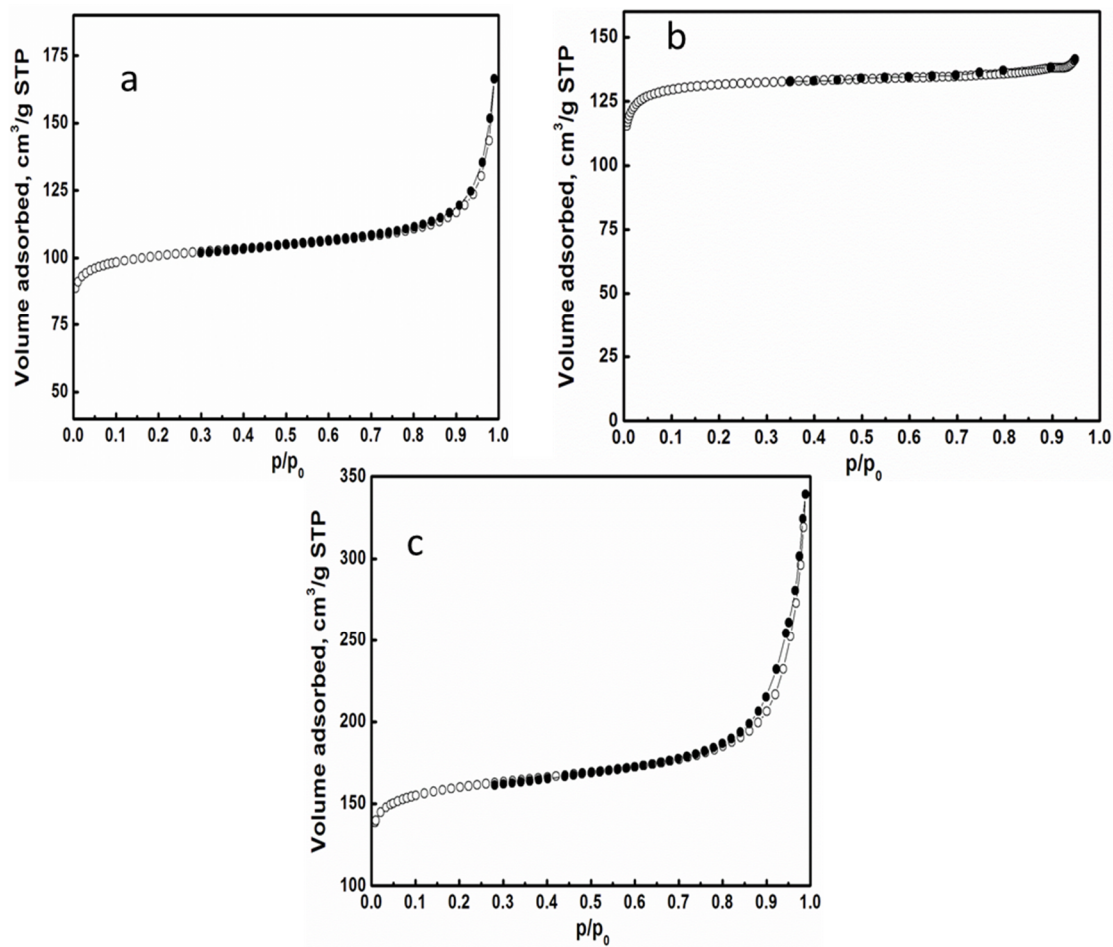


Figure 5.3 Nitrogen adsorption (\circ) and desorption (\bullet) isotherms of (a) IM-5 (b) TNU-9 (c) SSZ-33

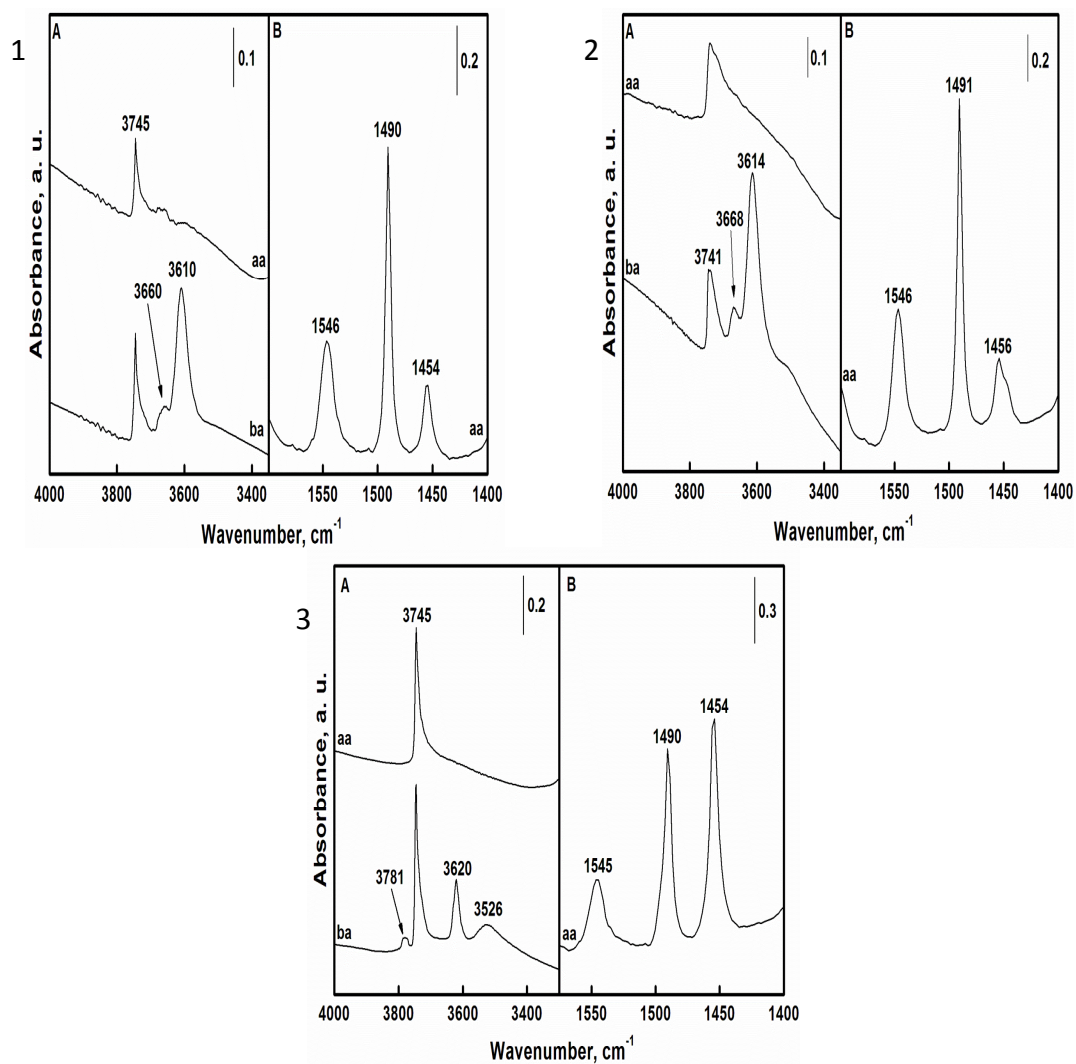


Figure 5.4 IR spectra of (1) IM-5 (2) TNU-9 (3) SSZ-33, adsorption of pyridine. Region of hydroxyl vibration (A), region of pyridine vibration (B). Before (ba) and after (aa) adsorption.

5.2.2 Catalytic activity

5.2.2.1 Ethylation of toluene

The dependence of toluene conversion on temperature is shown in Fig. 5.5 for the alkylation of toluene with ethanol on TNU-9, SSZ-33, MOR-18, IM-5 and ZSM-5. As expected, increase in temperature caused a rise in conversion over all the zeolites and the order of toluene conversion was $\text{TNU-9} > \text{IM-5} > \text{SSZ-33} > \text{MOR-18} > \text{ZSM-5}$ at the reaction conditions studied. The fact that the order didn't change significantly with reaction conditions depict that it is the zeolite characteristics that confers the degree of aromatic conversion. These characteristics could be the nature and strength of the acid sites or the ease with which the toluene molecules gain access into the channel system of the zeolites but from what is obtainable in the literature, it appears not only one but a combination of these factors are responsible. Odedairo et. al. [25] commented on toluene conversion during its disproportionation that it does not necessary go in line with the order of the zeolite's channel sizes and dimensionality, a point that was also strengthened by Zilkova et. al. [73]. The most unusual behavior observed was over MOR-18, one would think that its 12-MR will make it offer unhindered access to the toluene molecules thus to have the highest conversion but since it is unidimensional unlike the 3D nature of the other zeolites, any pore blocking caused by coke deposition results in a severe loss of activity in MOR-18 structure.

The total ET yield showed different behavior over the zeolites when studied with temperature and time as shown in Table 5.2, Table 5.3 and Fig. 5.6 respectively. For TNU-9 and IM-5 with similar channel dimensions in addition to MOR-18 with large pores, ET yield decreased with increase in temperature in contrast to SSZ-33 and ZSM-5,

which showed an increase at lower temperature, reached a maximum value at 300 °C then decreased with temperature. The decrease in ET yield at higher temperature over all the zeolites could be attributed to the decomposition of ethanol and disproportionation of toluene into benzene and xylenes.

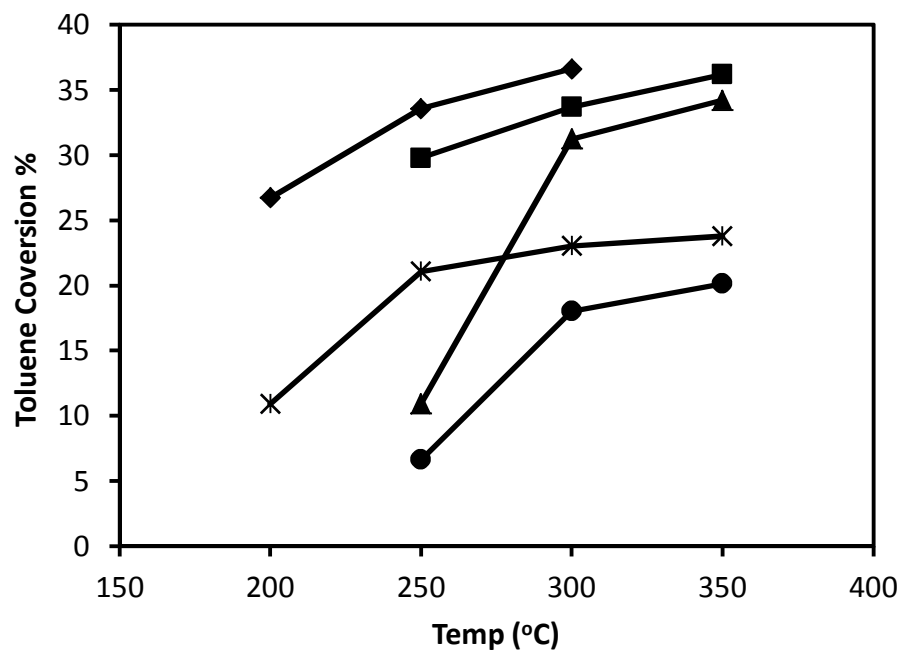


Figure 5.5 Effect of temperature on toluene conversion over TNU-9 (♦), IM-5 (■), SSZ-33 (▲), ZSM-5 (●) and MOR-18 (⋈) at reaction time of 20 s.

Table 5.2

Product distribution for toluene alkylation with ethanol at 20 s reaction time and 1:1 toluene: ethanol molar ratio for TNU-9, SSZ-33 and IM-5 zeolites

Catalyst	TNU-9			SSZ-33			IM-5		
Reaction Temp. (°C)	250	300	350	250	300	350	250	300	350
Toluene conversion (%)	33.6	36.6	32.8	10.9	31.2	34.2	29.8	33.7	36.2
Product yield (%)									
p-ET	2.0	1.3	0.7	2.2	3.9	2.8	3.7	3.1	2.2
m-ET	4.7	3.2	1.8	3.9	9.0	6.7	8.3	7.1	5.2
o-ET	0.9	0.7	0.4	2.6	2.3	1.7	1.7	1.6	1.3
Total-ET	7.6	5.2	2.9	8.6	15.2	11.2	13.7	11.8	8.6
Benzene	8.4	0.8	2.5	0.2	2.1	4.1	2.9	5.5	8.6
Ethylbenzene	5.1	1.5	1.8	0.6	4.4	4.7	4.7	5.0	4.5
Xylenes	10.1	2.0	3.36	1.0	6.7	10.9	6.6	9.6	12.5
DEBs + TMBs	2.3	0.9	0.7	0.5	2.8	3.4	1.9	1.9	2.0
ET selectivity (%)	22.7	14.1	8.7	78.9	48.6	32.8	46.0	34.9	23.9
p-ET selectivity (%)	26.3	25.0	24.9	25.1	25.8	25.2	27.3	26.5	25.3

Table 5.3

Product distribution for toluene alkylation with ethanol at 20 s reaction time and 1:1 toluene: ethanol molar ratio for ZSM-5 and MOR-18 zeolites

Catalyst	ZSM-5			MOR-18		
Reaction Temp. (°C)	250	300	350	250	300	350
Toluene conversion (%)	6.7	18.0	20.2	21.1	23.0	23.8
Product yield (%)						
p-ET	2.0	4.2	3.9	2.6	2.2	1.3
m-ET	3.3	8.4	7.8	6.5	5.5	3.2
o-ET	0.3	1.2	1.2	1.8	1.4	0.8
Total-ET	5.6	13.7	12.9	10.9	9.1	5.3
Benzene	0.1	0.6	1.4	1.5	2.6	4.2
Ethylbenzene	0.4	1.5	2.0	2.8	3.2	2.7
Xylenes	0.3	1.6	3.3	4.2	6.7	10.0
DEBs + TMBs	0.2	0.6	0.5	1.7	1.4	1.5
ET selectivity (%)	84.5	76.2	64.1	51.8	39.6	22.5
p-ET selectivity (%)	35.1	30.5	30.0	24.1	24.2	24.3

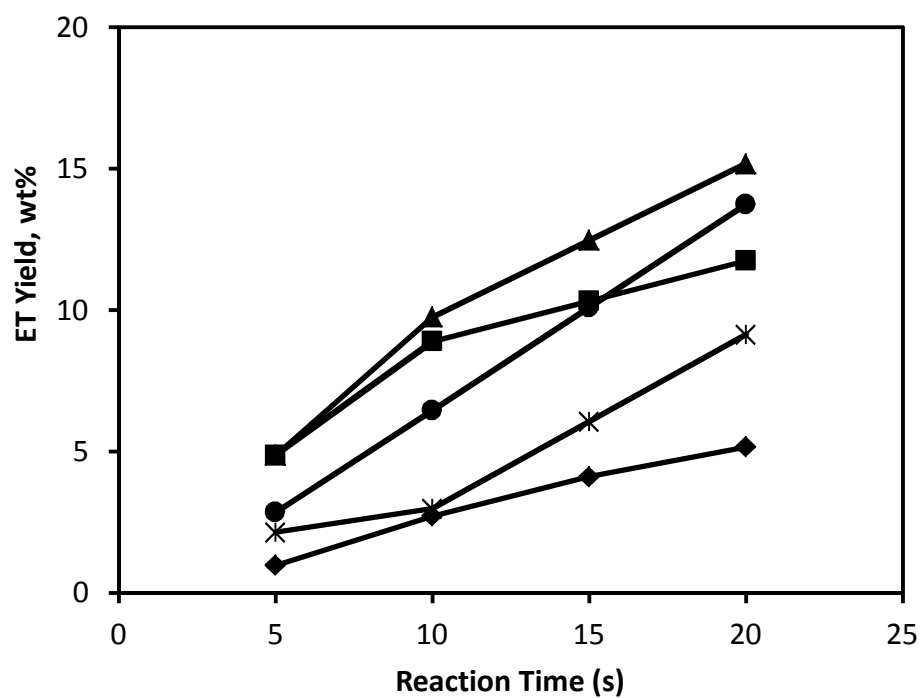


Figure 5.6 Effect of time on Ethyltoluene (ET) yield during toluene ethylation over TNU-9 (♦), IM-5 (■), SSZ-33 (▲), ZSM-5 (●) and MOR-18 (⋈) at Temperature = 300 °C.

The results obtained for toluene ethylation at different temperatures over all the five zeolites are detailed in Table 5.2 and 5.3. The observed product distribution consist mainly of ET isomers, benzenes and xylenes from toluene disproportionation, and some amounts of secondary alkylation products i.e. diethylbenzenes (DEB) and trimethylbenzenes (TMB) were obtained especially over zeolite with intersecting 12-MR; SSZ-33. This can be attributed to the restriction offered to these bulkier di- and tri-alkyl benzenes in zeolites with 10-rings. MOR-18 might have given more amounts of DEB and TMB but its high Brønsted sites could have enhanced their transformation into simpler aromatics. It is believed that alkylation reaction involving aromatic compounds is governed by carbenium ion type mechanism with the direct attachment of the alkylation agent to ortho-para position on the benzene ring followed by isomerization [11]. The strong (Brønsted) acid site of the zeolite sample adsorb and protonates an ethanol molecule to form ethyl oxonium ion before it is transformed to ethyl cation. This can then attach to toluene at either of ortho- or para- to form ET because of the available methyl group in toluene and depending on the channel size of the zeolite used.

Fig. 5.7 presents the ET selectivity during toluene ethylation over TNU-9, SSZ-33, IM-5, MOR-18 and ZSM-5. The zeolites showed similar trend in behavior towards ET selectivity and follow the order $ZSM-5 > MOR-18 > SSZ-33 > IM-5 > TNU-9$. MOR-18 and SSZ-33 with larger pore sizes than others showed more amount of o-ET, which is the largest in terms of diameter among all the isomers of ET, in their product distribution thus contributing to the observed ET-selectivity. For p-ET selectivity, ZSM-5 showed the highest due to its known shape-selectivity which occurs in the zeolite pore channels [28]

forming p-ET and then it undergoes isomerization to the other isomers on the available external surface acid sites.

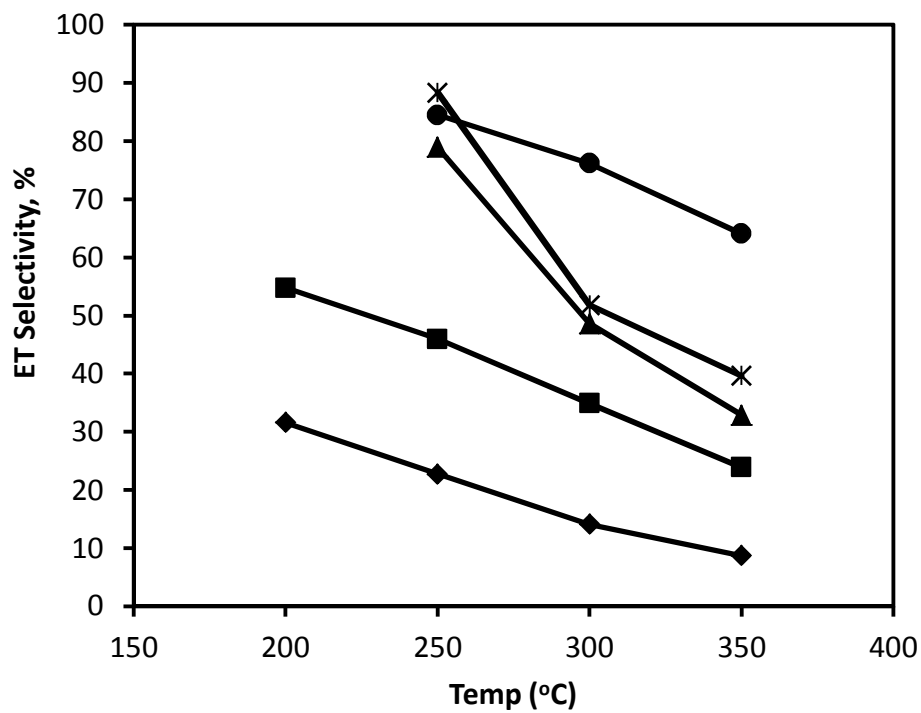


Figure 5.7 Effect of temperature on Ethyltoluene (ET) Selectivity during toluene ethylation over TNU-9 (◆), IM-5 (■), SSZ-33 (▲), ZSM-5 (●) and MOR-18 (X) at reaction time of 20 s.

5.2.2.2 Methylation of ethylbenzene

The alternative path to producing ETs that was also carried out was alkylation of EB with methanol. This will provide us with information about the possible effect of increasing the alkyl substituent on the aromatic ring as well as reducing the size of the alkylating agent in contrast with toluene ethylation. For EB conversion as shown in Fig. 5.8, ET yield in Fig. 5.9 and ET selectivity in Fig. 5.10, it could be observed that the zeolites showed the same order of activity as in toluene ethylation although EB conversion was higher compared to toluene conversion except over MOR-18. This could show that the bulkier the alkyl group on the aromatic ring becomes, the more active it will be in alkylation reactions because of the relative ease with which it could be substituted.

EB methylation gave a vast distribution of products similar to toluene ethylation on all the zeolites studied with a higher proportion of secondary alkylation products such as DEB and TMB. The entire products are shown in Table 3. Ko and Huang [13] in their related study, proposed a possible reaction pathway for the EB-methanol reaction. They assert that the primary reactions are disproportionation and methylation of EB to give DEB/benzene and ET respectively with the observed benzene and toluene arising from the dealkylation of EB and ET due to temperature effect. Some of the benzene can then react with methanol to give more toluene and the presence of xylene could suggest that some of the toluene subsequently undergoes disproportionation reaction. These multiple reactions occurring during alkylation of EB with methanol leads to a wide range of alkyl aromatics and results in a reduced formation of the product of interest i.e. ET thus making this reaction route not as selective to ET as alkylation of toluene with ethanol. This is evident in that the highest ET- selectivity obtained for the reaction was 40.1 %

over ZSM-5 compared to 84.5 % over the same ZSM-5 for toluene alkylation with ethanol. The kinetics section of this present work therefore will be focused on toluene ethylation and not EB-methanol reaction.

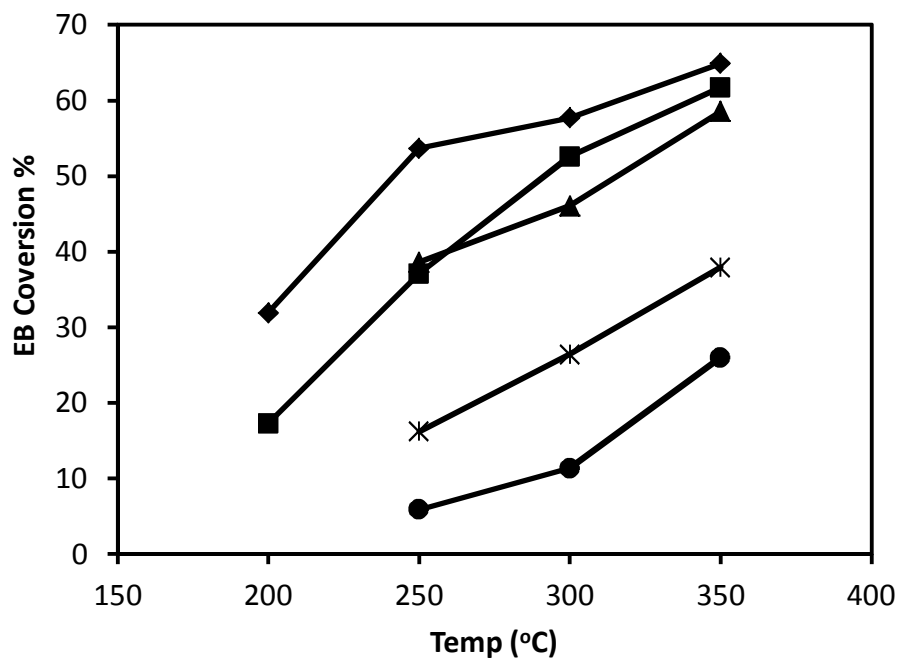


Figure 5.8 Effect of temperature on Ethylbenzene conversion over TNU-9 (♦), IM-5 (■), SSZ-33 (▲), ZSM-5 (●) and MOR-18 (✕) at reaction time of 20 s.

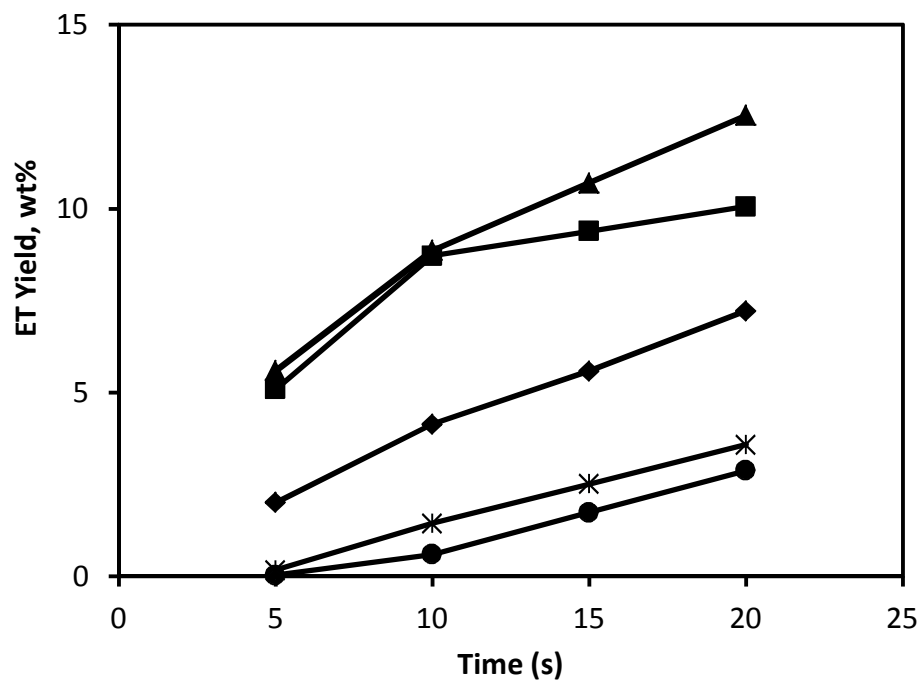


Figure 5.9: Effect of time on Ethyltoluene (ET) yield during ethylbenzene methylation over TNU-9 (◆), IM-5 (■), SSZ-33 (▲), ZSM-5 (●) and MOR-18 (✕) at Temperature = 300 °C.

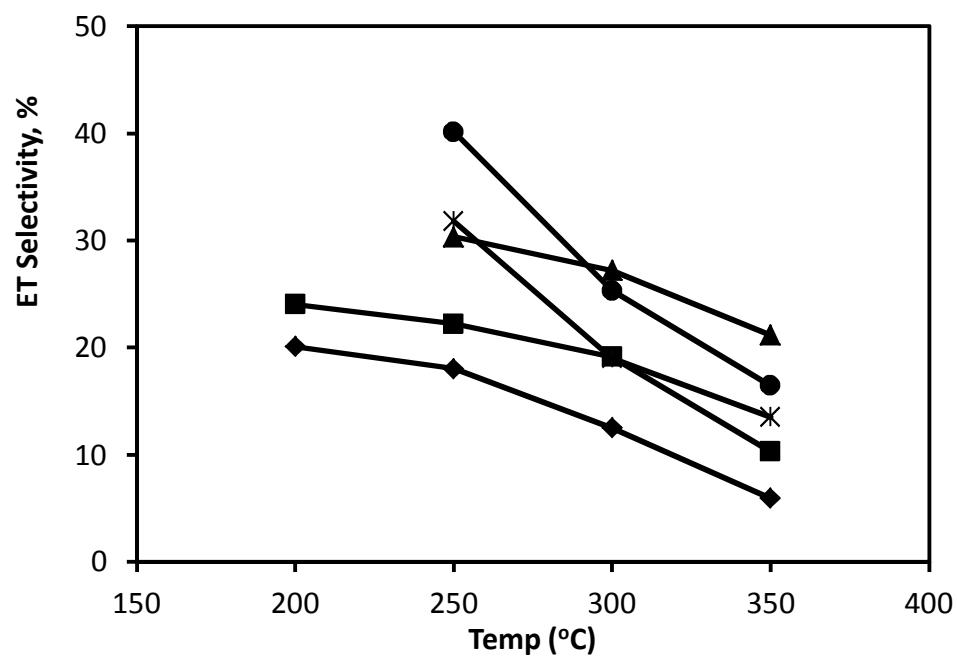


Figure 5.10 Effect of temperature on Ethyltoluene (ET) Selectivity during ethylbenzene methylation over TNU-9 (♦), IM-5 (■), SSZ-33 (▲), ZSM-5 (●) and MOR-18 (⋈) at reaction time of 20 s.

Fig. 5.11 and 5.12 compares the ET-selectivity and p-ET selectivity for all the zeolites at ~30% aromatic conversion respectively via both toluene ethylation and EB methylation reactions. Alkylation of toluene with ethanol showed higher ET-Selectivity compared to Ethylbenzene methylation but p-ET selectivity was almost same irrespective of the alkylation route or zeolite channel type. Taking ZSM-5 as a case-study, its p-ET selectivity for both alkylation reactions was almost 27%, which is quite close to the equilibrium composition [1]. Similar trend of alkylation reaction influencing ET yield was also observed in the zeolite samples as well. This could be attributed to the difference in the stability of the attacking alkyl group. Ethyl cation could be formed easily from ethanol than methyl cation from methanol. This could provide another explanation why higher ET-selectivity could be obtained from alkylation of toluene with ethanol.

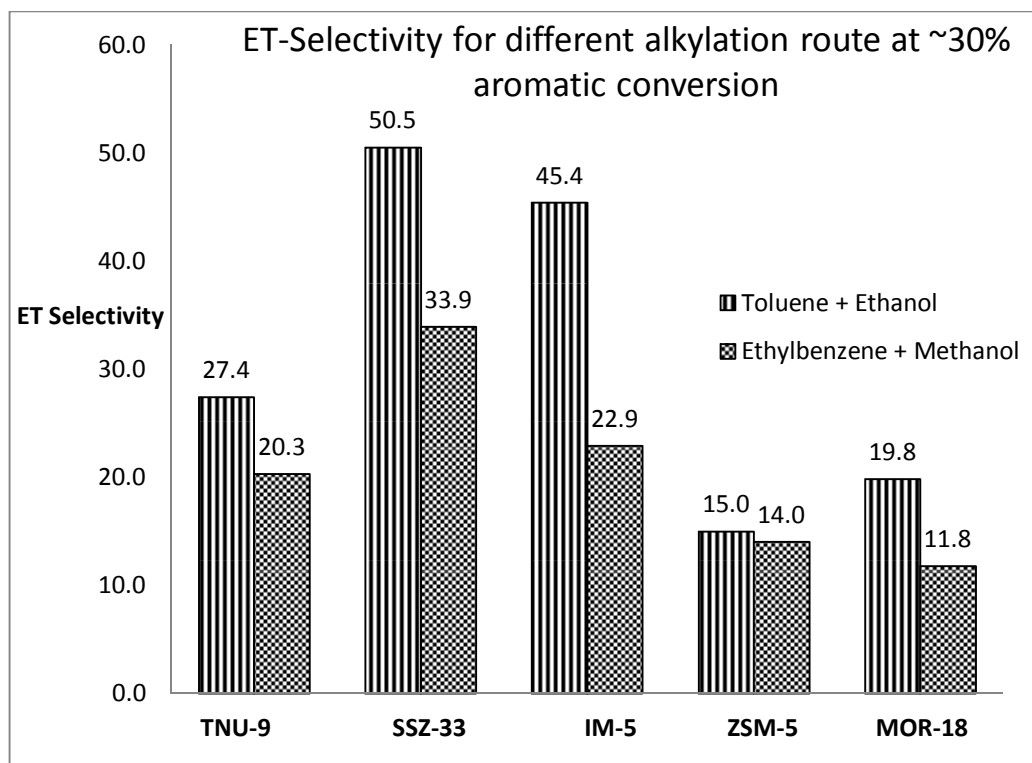


Figure 5.11 ET-Selectivity for different alkylation route at ~30% aromatic conversion

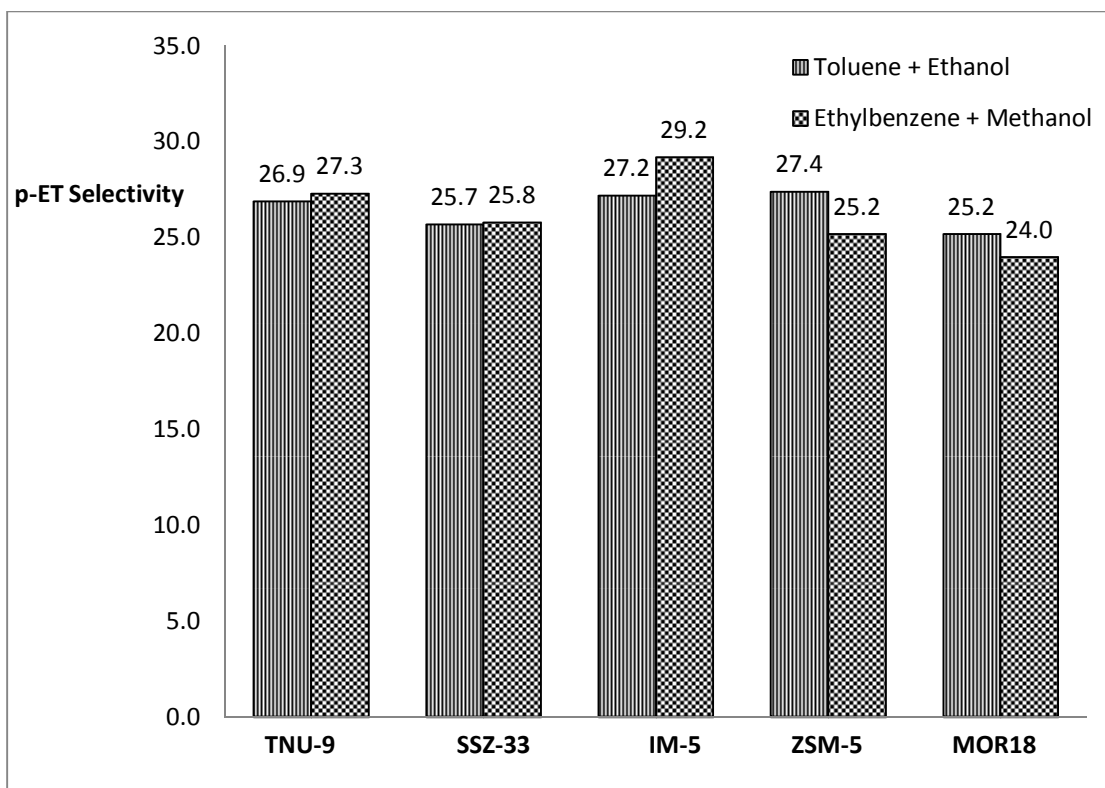


Figure 5.12 p-ET Selectivity for different alkylation route at ~30% aromatic conversion

Over TNU-9, the most abundant products were benzene and xylene. It is unclear if this is due to its acidity or channel system perhaps a combination of both because nearly the same result would have been expected over ZSM-5 if it were due to its channel system alone. SSZ-33 gave more of the bulky products such as DEB and TMB when compared to the other 3-D zeolites. This is due to the higher diffusion coefficient of DEB and TMB, a condition favored by the wider channels of SSZ-33.

5.3 Kinetics of Toluene alkylation with ethanol

The kinetics involved in the reaction between toluene and ethanol in a riser simulator was studied using mathematical models that represent the rate expressions for the reactants consumption and products formation, taking into consideration all the possible limitations that usually accompany any catalytic process. The operating conditions were assumed to be isothermal based on the design of the reactor unit and the relatively small amount of reactants used in the study. The rate expressions for toluene ethylation were assumed to obey second-order kinetics and a pseudo-first order reaction kinetic was used for all components involved in the reaction. Catalyst deactivation is taken to be a function of reaction time, and a single deactivation function was defined for all reactions. Using the design equation for a batch reactor with the power law rate equation, the rate of chemical reaction can be written as:

$$\frac{V}{W_c} \frac{dC_i}{dt} = r_i \exp(-at)$$

where r_i and C_i are the reaction rate and molar concentration of the species in the system, V is the volume of the riser simulator, W_c is the mass of the catalyst used, t is time in

seconds and $\exp(-\alpha t)$ is the catalyst deactivation function (Time on Stream model) which accounts for catalytic activity loss and α is known as the catalyst decay constant. Molar concentration, C_i , can be expressed in terms of weight fraction of each species y_i , which are the measurable variables from the chromatographic analysis, we have:

$$C_i = \frac{y_i W_{hc}}{MW_i V}$$

where W_{hc} is the weight of reactant injected into the reactor, MW_i is the molecular weights of the species.

The reaction rate, r_i , is a function of the rate constant and the concentration of the reacting species. The temperature dependency of rate constant, k_i , is given in terms of Arrhenius equation as:

$$k_i = k_{i0} \exp \left[-\frac{E_i}{R} \left(\frac{1}{T} - \frac{1}{T_0} \right) \right]$$

where k_{i0} is the pre-exponential factor of reaction i and E_i is the energy of activation of the reaction i . T_0 is referred to as the centering temperature, obtained as the average of all the temperatures used in the experiment to reduce parameter interaction as stated by Agarwal and Brisk [74].

5.3.1 Reaction Mechanism

A simplified reaction path for toluene alkylation with ethanol to products is represented as shown in Figure 5.13 based on the product distribution observed over the zeolites. DEB and TMB were not accounted for because their amount is relatively small compared to other products and accounting for them will unnecessarily complicate the modelling by adding more parameters that needs fitting.

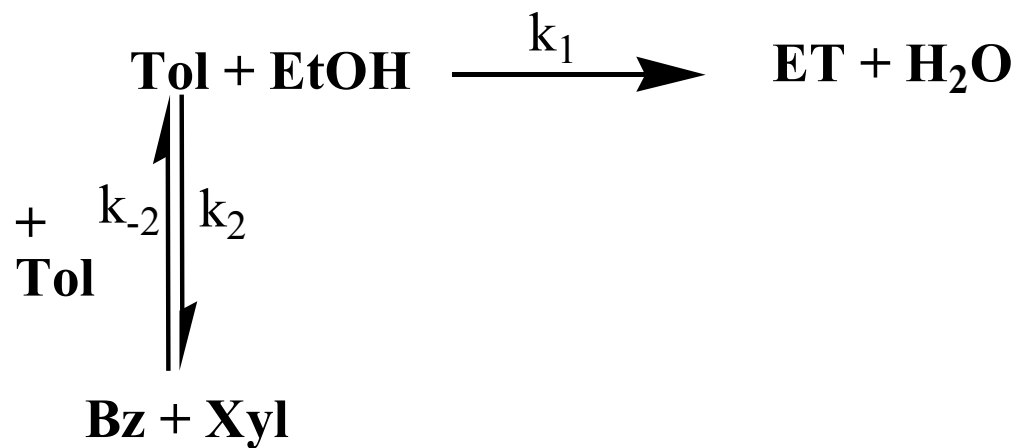


Figure 5.13 Simplified Reaction path for toluene ethylation

Rate of Toluene consumption

$$\frac{-V}{W_c} \frac{dC_T}{dt} = \eta(k_1 C_T C_E + k_2 C_T^2 - k_{-2} C_{Bz} C_X) \exp(-\alpha t)$$

Rate of Ethyltoluene formation

$$\frac{V}{W_c} \frac{dC_{ET}}{dt} = \eta k_1 C_T C_E \exp(-\alpha t)$$

Rate of Benzene formation

$$\frac{V}{W_c} \frac{dC_{Bz}}{dt} = \eta(k_2 C_T^2 - k_{-2} C_{Bz} C_X) \exp(-\alpha t)$$

Rate of Xylene formation

$$\frac{V}{W_c} \frac{dC_X}{dt} = \eta(k_2 C_T^2 - k_{-2} C_{Bz} C_X) \exp(-\alpha t)$$

Like any catalytic process, alkylation of toluene with ethanol also involves the bulk diffusion of reactants to the external surface of the catalyst, pore diffusion to the active sites, and reaction on the catalytic surface. Any of these steps could be the limiting step and as such must be accounted for in modelling the entire process.

To check if bulk transport limitation occurs during the reaction, Frössling's correlation [75] could be employed

$$Sh = 2 + 1.1 Sc^{0.33} Re^{0.6}$$

$$k_c = \frac{Sh D_{Tol,Ar}}{d_p}$$

$$\Delta C = C_{tol,b} - C_{tol,s} = \frac{-r''_{tol,obs}}{k_c}$$

Where Sh is Sherwood number, Sc is Schmidt number, Re is Reynolds number, d_p is particle diameter, $C_{tol,b}$ is toluene concentration in the bulk, $C_{tol,s}$ is toluene concentration at the catalyst surface, k_c is mass transfer coefficient, $D_{tol,Ar}$ is diffusivity of toluene in argon

The diffusivity of toluene in argon can be estimated using either the Fuller, Schettler and Giddings correlation or by that provided by Bird et al. [76].

The Frössling's correlation can be evaluated with the assumption that the shear stress over the catalyst is negligible because the average particle size of the catalysts is small (30 μm). This literally corresponds to the highest film resistance obtainable and the Froessling correlation can be approximated to $Sh = 2$.

The observed rate of reaction for toluene can be calculated using the expression

$$-r''_{tol,obs} = \frac{N_{tol0}X_{tol}}{W S_{ex} t}$$

N_{tol0} is the initial number of moles of toluene, X_{tol} is the conversion of toluene, W is the weight of catalyst, t is the time taken for the reaction and S_{ex} is the external surface area per gram of catalyst.

Once the observed rate and mass transfer coefficient have been calculated, the change in concentration from the bulk to the surface of the catalyst can be evaluated then judgement can be taken if mass transfer limits the process.

For internal diffusion limitation, it can be evaluated by using the Weisz-Prater criterion. Internal diffusion can be ignored if the condition is satisfied

$$C_{WP} = \frac{-r_{tol(obs)}\rho_p R_p^2}{D_e C_{tol,s}} \ll 1$$

From Table 4 and Table 5, the value of ΔC_{film} and CWP obtained at the various operating condition are very small. A small ΔC_{film} means that there is no appreciable concentration gradient from the bulk to the surface of the catalyst i.e. no external diffusion limitation and CWP showed that internal diffusion does not hinder the reaction. Since it has been established that neither external nor pore diffusion limits the reaction, the effectiveness factor can be given a value of 1 and the kinetics can accurately be predicted by the rate expressions.

The reaction schemes contains several parameters which were determined by using non-linear regression (MATLAB LSQCURVEFIT) to fit the experimental data into the rate expressions and their values with 95 % confidence limits are given in Table 5.

Table 5.4:

Evaluating effect of external diffusion limitation

Temperature (°C)	$D_{\text{tol,Ar}}$ (m^2/s)	k_c (m/s)	Time (s)	$-r_{\text{tol(obs)}}$ ($\text{mole}/\text{m}^2\text{s}$)	$C_{\text{tol,b}}$ (mol/m^3)	ΔC_{film} (mol/m^3)
250	2.15×10^{-5}	1.43	20	5.15×10^{-5}	26.1	3.59×10^{-5}
300	2.54×10^{-5}	1.69	20	5.83×10^{-5}	26.1	3.44×10^{-5}
350	2.95×10^{-5}	1.97	20	6.26×10^{-5}	26.1	3.18×10^{-5}

Table 5.5:

Evaluating effect of internal diffusion limitation

Temperature (°C)	D _{eff} (m ² /s)	Time (s)	-r _{tol(obs)} (mole/kg.s)	C _{tol,s} (mol/m ³)	CWP
200	2.15 x 10 ⁻⁵	20	18.4	26.1	1.05 x 10 ⁻⁵
250	2.54 x 10 ⁻⁵	20	20.8	26.1	7.33 x 10 ⁻⁶
300	2.95 x 10 ⁻⁵	20	22.3	26.1	8.07 x 10 ⁻⁶

5.3.2 Model parameter evaluation

The kinetic parameters (k_{oi} , E_i , α) for the alkylation reaction of toluene with ethanol were estimated by non-linear regression analysis coupled with fourth order Runge-Kutta in the integration of the rate expressions numerically. The models provide approximate estimates of all the kinetic parameters which are detailed in Table 5.6. The proposed reaction mechanism was tested by comparing the experimental data with the results predicted by the model using the fitted parameters and a good correlation was obtained with the R^2 value close to unity (0.98).

It can be observed that based on the activation energies of the zeolites used in this study, IM-5 (58.2 kJ/mol) > SSZ-33 (39.7 kJ/mol) > TNU-9 (27.3 kJ/mol) > MOR-18 (20.2 kJ/mol) > ZSM-5 (17.0 kJ/mol). Most kinetic studies that have been reported for toluene ethylation in the literature are over ZSM-5 zeolite thereby limiting the scope of comparison but similar reactions could also be used. Odedairo et. al. [25] reported activation energy of 17.1 kJ/mol during toluene disproportionation and 33.9 kJ/mol during toluene methylation over TNU-9. They also worked on SSZ-33 and MOR zeolites for alkylation reaction between toluene and methanol. Lee and Wang [27] used ZSM-5 ($\text{SiO}_2/\text{Al}_2\text{O}_3 = 90$) for alkylation of toluene with ethylene and obtained a value of 75 kJ/mol. It would be expected that the ZSM-5 used in this study should have a lower apparent activation energy due to its lower $\text{SiO}_2/\text{Al}_2\text{O}_3$ ratio because apparent activation energy is half the summation of intrinsic and diffusion activation energies, i.e. $E_{app} = \frac{E_i + E_d}{2}$ [77]. The intrinsic activation energy of a catalyst depends on the acid strength which could be indicated by its $\text{SiO}_2/\text{Al}_2\text{O}_3$ ratio.

Table 5.6
Estimated kinetic parameters for toluene ethylation on different zeolites

Parameters	MOR-18	ZSM5	TNU-9	SSZ-33	IM-5
$k_{\theta 1} * 10^2$ ($m^6/kgcat.s$)	0.237 ± 0.1	0.146 ± 0.02	0.849 ± 0.03	0.662 ± 0.07	0.129 ± 0.06
E_1	20.2 ± 9.7	17.0 ± 6.0	27.3 ± 0.73	39.7 ± 9.1	58.2 ± 16.3
$k_{\theta 2} * 10^2$ ($m^6/kgcat.s$)	0.327 ± 0.09	0.479 ± 0.03	0.52 ± 0.17	0.947 ± 0.07	0.26 ± 0.04
E_2	8.4 ± 0.73	26.1 ± 1.0	10.3 ± 1.1	46.0 ± 11.3	20.2 ± 1.4
$k_{-\theta 2} * 10^2$ ($m^6/kgcat.s$)	29.1 ± 5.1	3.8 ± 0.1	5.52 ± 0.87	0.25 ± 0.09	27.7 ± 2.6
E_{-1}	42.2 ± 6.6	44.3 ± 7.9	44.2 ± 6.3	39.8 ± 3.8	53.5 ± 4.5
α	0.15 ± 0.03	0.21 ± 0.07	0.14 ± 0.03	0.07 ± 0.01	0.04 ± 0.01

CHAPTER SIX

CONCLUSIONS AND RECOMMENDATIONS

6.1 Conclusions from MFI comparative study

The ethylation of toluene with ethanol over MFI-zeolites of varying $\text{SiO}_2/\text{Al}_2\text{O}_3$ ratio and crystal size has been investigated with detailed kinetic modeling. The following conclusions could be drawn:

1. The activity of MFI zeolites for toluene ethylation is a function of concentration and strength of acid sites, highest activity was observed over MFI-80 with more strong acid sites, while para-selectivity is associated with both crystal size and $\text{SiO}_2/\text{Al}_2\text{O}_3$ ratio, displayed by MFI-2000. No catalytic activity or selectivity was observed over silicalite-1.
2. MFI-2000 yielded the highest p-ET selectivity (100%) due to its low-acidity and external surface area thus preventing the isomerization of p-ET into m-ET.
3. Benzene and xylenes, which are products of toluene disproportionation, were observed over MFI-80 and MFI-280 but not over MFI-2000 due to the presence of Brønsted acid sites aiding toluene disproportionation.
4. Based on Langmuir-Hinshelwood mechanism for toluene ethylation, a model with both ethanol and ethyltoluenes adsorbed on the catalyst surface sites best fits the experimental data.

5. MFI-280 required the lowest amount of activation energy to form p-ET which is attributed to its higher acidic content and higher activity compared with MFI-2000.

6.2 Conclusions from different zeolites and alkylation routes

Five zeolites with different channel systems and pore sizes (TNU-9, IM-5, SSZ-33, MOR-18, and ZSM-5) were used in studying the alkylation reactions involving toluene/ethylbenzene and ethanol/methanol respectively using a fluidized bed reactor. Their activity was found to follow the order; TNU-9 > IM-5 > SSZ-33 > MOR-18 > ZSM-5, without any significant change with reaction conditions and alkylation route. Methylation of EB in comparison with ethylation of toluene under the same reaction conditions resulted in a lower selectivity to ET although p-ET selectivity was almost the same irrespective of the nature of zeolite and reaction used.

Kinetics of the toluene alkylation reaction modeled by power law is well represented by the two-step reaction mechanism. The activation energies for ET formation were found in the order; IM-5 (58.2 kJ/mol) > SSZ-33 (39.7 kJ/mol) > TNU-9 (27.3 kJ/mol) > MOR-18 (20.2 kJ/mol) > ZSM-5 (17.0 kJ/mol). These values do not correspond with the order of pore dimension of the catalysts.

6.3 Recommendation

Sequel to the results obtained in this thesis work, the following recommendations could be made;

- Further work should be done on ZSM-5 so as to improve the p-ET yield. This work has achieved 100 % selectivity but the amount produced is another critical factor if it is to gain the much needed industrial success.

- Modification of SSZ-33 should be carried out because it showed high ET selectivity. There is possibility of attaining better yield of p-ET if the isomerization occurring in the SSZ-33 can be minimized.

NOMENCLATURE

C_i	concentration of specie i in the riser simulator (mol/m ³)
CL	confidence limit
E_i	apparent activation energy of the i th reaction (kJ/mol)
K_i	adsorption equilibrium constant of component i
k_i	apparent rate constant for the i th reaction (m ³ /kg of catalyst .s)
k_{oi}	pre-exponential factor for i th reaction after re-parameterization
MW_i	molecular weight of specie i
R	universal gas constant (kJ/kmol K)
t	reaction time (s)
T	reaction temperature (K)
T_o	average temperature of the experiment (K)
V	volume of the riser (45 cm ³)
W_c	mass of the catalyst (0.81 g)
W_{hc}	total mass of the hydrocarbon injected the riser (0.162 g)
$\Delta S_{ads,i}^0$	entropy for adsorption for componenet i
$\Delta H_{ads,i}^0$	enthalpy for adsorption for componenet i

Greek Letters

φ	apparent deactivation function
-----------	--------------------------------

α catalyst deactivation constant (Time on stream model)

Abbreviations

DEB diethylbenzene

EB ethylbenzene

ET ethyltoluenes

EtOH ethanol

m-ET meta-ethyltoluene

MOR mordenite

TMB trimethylbenzene

p-ET para-ethyltoluene

o-ET ortho-ethyltoluene

IZA International Zeolite Association

REFERENCES

- [1] W.W. Kaeding, L.B. Young, C-C. Chu, *J. Catal.* 89 (1984) 267-273.
- [2] J. Čejka, B. Wichterlová, *Catal. Rev. Sci. Eng.* 44 (2002) 375-421.
- [3] J. Walendziewski, J. Trawczyński, *Ind. Eng. Chem. Res.* 35 (1996) 3356-3361.
- [4] F. Lónyi, J. Engelhardt, D. Kalló, 11 (1991) 169-177.
- [5] N.E. Villareal, B.I. Kharisov, I.I. Ivanova, B.V. Romanovskii, *Appl. Catal. A: Gen.* 224 (2002) 161-166.
- [6] Lidback, A.A., *Aromatics Update*. 2012: Presented at Pemex Petrochemical Forum.
- [7] V.N. Romannikov, K.G. Ione, *J. Catalysis*. 146 (1994) 211-217.
- [8] G. Paparatto, E. Moretti, G. Leofanti, F. Gatti, *J. Catal.* 105 (1987) 227-232.
- [9] V. Bhandarkar, S. Bhatia, *Zeolites* 14 (1994) 39-49.
- [10] P.A. Parikh, *Ind. Eng. Chem. Res.* 47 (2008) 1793-1797.
- [11] R. Manivannan, A. Pandurangan, *Kinet. Catal.* 51 (2010) 56-62.
- [12] J. Engelhardt, D. Kalló, I. Zsinka, *J. Catal.* 135 (1992) 321-324.
- [13] A. N. Ko, C.S. Huang, *J. Chin. Chem. Soc.* 40 (1993) 345-350.
- [14] F. J. Llopi, G. Sastre, A. Corma, *J. Catal.* 227 (2004) 227-241.
- [15] J. Shin, S.B. Hong, *Micro Meso Mater.* 124 (2009) 227-231.
- [16] Ch. Baerlocher, F. Gramm, L. Massüger, L.B. McCusker, Z. He, S. Hovmöller, X. Zou, *Science*, 315 (2007) 1113-1116.
- [17] A. Corma, J. Martínez-Triguero, S. Valencia, E. Benazzi, S. Lacombe, *J. Catal.* 206 (2002) 125-133.
- [18] S.H. Lee, D.K. Lee, C.H. Shin, Y.K. Park, P.A. Wright, W.M. Lee, S.B. Hong, *J. Catal.* 215 (2003) 151-170.
- [19] N. He, H.B. Xie, Y.H. Ding, *Micro Meso Mater.* 121 (2009) 95-102.
- [20] A.E. Palomares, J.G. Prato, A. Corma, *Ind. Eng. Chem. Res.* 42 (2003) 1538-1542.
- [21] F. Bleken, W. Skistad, K. Barbera, M. Kustova, S. Bordiga, P. Beato, U. Olsbye, *Phys. Chem. Chem. Phys.*, 13 (2011) 2539-2549.
- [22] G.D. Lei, B.T. Carvill, W.M.H. Sachtler, *Appl. Catal. A*, 42 (1996) 347-359

- [23] C. Shao, H.Y. Kim, X. Li, S.J. Park, D.R. Lee, *Mater. Lett.*, 56 (2002) 24–29
- [24] T. Odedairo, S. Al-Khattaf, *Chem. Eng. J.* 157 (2010) 204-215.
- [25] T.Odedairo, R.J. Balasamy, S. Al-Khattaf, *Ind. Eng. Chem. Res.* 50 (2011) 3169-3183.
- [26] I.K. Wang, B.J. Lee, M.H. Chen, US Patent No. 4849386 (1989).
- [27] B.-J. Lee, I. Wang, *Ind. Eng. Chem. Prod. Res. Dev.* 24 (1985) 201-205.
- [28] G. Paparatto, G. De Alberti, G. Leofanti, M. Padovan, *Stud. Surf. Sci. Catal.* 44 (1989) 255-263.
- [29] W.W. Kaeding, G. Barile, Springer US. (1984) 267-273.
- [30] P.A. Parikh, N. Subrahmanyam, Y.S. Bhat, A.B. Halgeri, *Catal. Lett.* 14 (1992) 107-213.
- [31] B. Wichterlová, J. Čejka, *Catal. Lett.* 16 (1992) 421-429.
- [32] H. Ban, S. Chang, W. Ahn, *Korean J. Chem. Eng.*, 40(2002) 139-145.
- [33] Wang, I., C. Ay, B. Lee, M. Chen, *Appl. Catal.*, 54 (1989) 257-266.
- [34] J. Cejka, N. Zilkova, B. Wichterlova, G. Eder-Mirth, J.A. Lercher, *Zeolites* 17 (1996) 265-271
- [35] B. Coughlan, W.M. Carroll, J. Nunan, *J. Chem. Soc.*, 79 (1983) 311-325.
- [36] C.S. Huang, A.N. Ko, *Catal. Lett.* 19 (1993) 319-326.
- [37] B. Rajesh, M. Palanichamy, V. Kazansky, V. Murugesan, *Indian J. Chem. A*, 40 (2001) 1262-1268.
- [38] V. Umamaheswari, C. Kannan, B.Mathiarabindoo, M. Palanichamy, V. Murugesan, *Proc. Indian Acad. Sci. Chem. Sci.* 112 (2000) 439-448.
- [39] M. Hartmann, S.P. Elangovan, *Adv. Nano. Mat.*, 2009, 236-311.
- [40] L.A. Atanda, A.M. Aitani, S.S. Al-Khattaf, *Chem. Eng. Res. Design* 95 (2015) 34-46.
- [41] G.D. Yadav, S.A. Purandare, *Micr. Meso. Mater.* 103 (2007) 363-372.
- [42] T. Odedairo, S. Al-Khattaf, *Chem. Eng. J.* 167 (2011) 240-254.
- [43] V. Bhandarkar, S. Bhatia, *Zeolites* 14 (1994) 39-49.
- [44] E.P. Barret, L.J. Joyner, P.H. Halenda, *J. Am. Chem. Soc.* 73 (1951) 373-380.

- [45] N. Žilková, B. Gil, S.I. Zones, S.J. Hwang, M. Bejblová, J. Čejka, Stud. Surf. Sci. Catal. 174 (2008) 1027-1032.
- [46] N. Žilková, M. Bejblová, B. Gil, S.I. Zones, A.W. Burton, C.Y. Chen, Z. Musilova, J. Čejka, J. Catal. 266 (2009) 79-91.
- [47] H.I. de Lasa, U.S. Patent No. 5102628, 1992.
- [48] K. Beschmann, L. Riekert, J. Catal. 141 (1993) 548-565.
- [49] T. Yashima, Y. Sakaguchi, S. Namba, Stud. Surf. Sci. Catal. 7 (1981) 739-751.
- [50] J. Nunan, J.A. Cronin, J. Cunningham, J. Am. Chem. Soc. 81 (1985) 2027-2041.
- [51] J. Čejka, A. Vondrová, B. Wichterlová, G. Vorbeck, R. Fricke, Zeolites 14 (1994) 147-153.
- [52] K.H. Chandavar, S.G. Hegde, S.B. Kulkarni, P. Ratnassamy, G. Chitlangia, A. Singh, A. Deo, Proceedings 6th Intl. Zeolite Conference, D. Olson and A. Bisio (Editors), Butterworth, Guilford, 1984, 325-330.
- [53] U.V. Mentzel, K.T. Højholt, M.S. Holma, R. Fehrmann, P. Beato, Appl. Catal. A: Gen. 417-418 (2012) 290-297.
- [54] K. Toch, J.W. Thybaut, B.D. Vandegehuchte, C.S.L. Narasimhan, L. Domokos, G.B. Marin, Appl. Catal. A: Gen. 425-426 (2012) 130-144.
- [55] M.M. Hossain, L. Atanda, N. Al-Yassir, S. Al-Khattaf, Chem. Eng. J. 207-208 (2012) 308-321.
- [56] J.M. Smith, H.C. Van Ness, M.M. Abbott, Introduction to Chemical Engineering Thermodynamics, 6th ed., McGraw-Hill, Boston, 2001.
- [57] S. Al-Khattaf, J.A. Atias, K. Jarosch, H. de Lasa, Chem. Eng. Sci. 57 (2002) 4909-4920.
- [58] S. Waziri, A. Aitani, S. Al-Khattaf, Ind. Eng. Chem. Res. 49 (2010) 6376-6387.
- [59] C. S. Triantafillidis, N. P. Evmiridis, L. Nalbandian, I.A. Vasalos, Ind. Eng. Chem. Res. 38 (1999) 916-927.
- [60] M.M.J. Treacy, J.B. Higgins, R. von Ballmoos, *Collection of Simulated XRD Powder Diffraction Patterns for Zeolites*, 4th Ed., Elsevier, London, 2001, p 237.
- [61] C.H. Baerlocher, W.M. Meier, D.H. Olson, Atlas of Zeolite Framework, 6th Ed., Elsevier Science, Amsterdam, 2007, p 212.
- [62] T.A.J. Hardenberg, L. Mertens, P. Mesman, H.C. Muller, C.P. Nicolaides, Zeolites, 12 (1992) 685-689.

- [63] N. Kadata, M. Niwa, *Catal. Surv. Asia* 8 (2004) 161-170.
- [64] M. Osman, L. Atanda, M.M. Hossain, S. Al-Khattaf, *Chem. Eng. J.* 222 (2013) 498-511.
- [65] N. Arsenova-Härtel, H. Bludau, R. Schumacher, W.O. Haag, H.G. Karge, E. Brunner, *J. Catal.* 191 (2000) 326-331.
- [66] D. Chen, K. Moljord, T. Fuglerud, A. Holmen, *Micro Meso Mater.* 29 (1999) 191-203.
- [67] N.Y. Chen, T.F. Degnan, C.M. Smith, *Molecular Transport and Reaction in Zeolites: Design and Application of Shape Selective Catalysis*, Wiley-VCH, Weinheim, 1994.
- [68] S. Al-Khattaf, *Ind. Eng. Chem. Res.* 46 (2007) 59-69.
- [69] P.J. Canteniro, US Patent 4,230,836, 1980
- [70] T. Hui, W. Jun, R. Xiaoqian, C. Demin, *Chin. J. Chem. Eng.* 19 (2011) 292-298.
- [71] J. Čejka, B. Wichterlová, S. Bednářová, *Appl. Catal. A: Gen.* 79 (1991) 215-226.
- [72] Y. He, T. C. Hoff, L. Emdadi, Y. Wu, J. Bouraima, D. Liu, *Catal. Sci. Technol.*, 4 (2014) 3064-3073.
- [73] N. Žilková, B. Gil, S.I. Zones, S.J. Hwang, M. Bejblová, J. Čejka, *Stud. Surf. Sci. Catal.* 174 (2008) 1027-1032.
- [74] A.K. Agarwal, M.L. Brisk, *Ind. Eng. Chem. Process Des. Dev.* 24 (1985) 203-207.
- [75] N. Frössling, *Gerlands Beitr. Geophys.* 52(1938) 170
- [76] R.B. Bird, W.E. Stewart, E.N. Lightfoot, *Transport Phenomena*. 2007: Wiley
- [77] O. Levenspiel, *Chemical Reaction Engineering*, John Wiley & Sons, New York, 1999.

VITAE

Name	Babatunde Azeez Ogunbadejo
Nationality	Nigerian
Date of Birth	29 th June 1986
Email	ogunbadejo.babatunde@yahoo.com
Address	19, Oduselu Street, Itire, Surulere, Lagos.
Academic Background	<p>M. Sc., Chemical Engineering from King Fahd University of Petroleum and Minerals, Dhahran, Saudi Arabia, May 2015.</p> <p>B. Eng, Chemical Engineering from Federal University of Technology, Minna, Nigeria, May 2012.</p> <p>National Diploma in Chemical Engineering from Lagos State Polytechnic, July 2005.</p>
Publication	B. Ogunbadejo, M. Osman, P. Arudra, A. Aitani, S. Al-Khattaf, “Alkylation of toluene with ethanol to para-ethyltoluene over MFI-zeolites: Comparative Study and kinetic modelling”, <i>Catalysis Today</i> , 243 (2015) 109–117